30. Bukreyev, A., Lamirande, E. W., Buchholz, U. J., Vogel, L. N., Elkins, W. R., St Claire, M., Murphy, B. R., Subbarao, K. & Collins, P. L. (2004) *Lancet* 363, 2122-7.
31. Babcock, G. J., Esshaki, D. J., Thomas, W. D., Jr. & Ambrosino, D. M. (2004) *J Virol* 78, 4552-60.
32. Buchholz, U. J., Bukreyev, A., Yang, L., Lamirande, E. W., Murphy, B. R., Subbarao, K. & Collins, P. L. (2004) *Proc Natl Acad Sci U S A* 101, 9804-9.
33. van den Brink, E. N., Ter Meulen, J., Cox, F., Jongeneelen, M. A., Thijsse, A., Throsby, M., Marissen, W. E., Rood, P. M., Bakker, A. B., Gelderblom, H. R., Martina, B. E., Osterhaus, A. D., Preiser, W., Doerr, H. W., de Kruif, J. & Goudsmit, J. (2005) *J Virol* 79, 1635-44.
34. Pogrebnyak, N., Golovkin, M., Andrianov, V., Spitsin, S., Smirnov, Y., Egolf, R. & Koprowski, H. (2005) *Proc Natl Acad Sci U S A* 102, 9062-7.
35. Ho, Y., Lin, P. H., Liu, C. Y., Lee, S. P. & Chao, Y. C. (2004) *Biochem Biophys Res Commun* 318, 833-8.
36. Mortola, E. & Roy, P. (2004) *FEBS Lett* 576, 174-8.
37. Huang, Y., Yang, Z. Y., Kong, W. P. & Nabel, G. J. (2004) *J Virol* 78, 12557-65.
38. Gao, W., Tamin, A., Soloff, A., D'Aiuto, L., Nwanegbo, E., Robbins, P. D., Bellini, W. J., Barratt-Boyes, S. & Gambotto, A. (2003) *Lancet* 362, 1895-6.
39. Ishii, K., Ueda, Y., Matsuo, K., Matsuura, Y., Kitamura, T., Kato, K., Izumi, Y., Someya, K., Ohsu, T., Honda, M. & Miyamura, T. (2002) *Virology* 302, 433-44.
40. Ishii, K., Hasegawa, H., Nagata, N., Mizutani, T., Morikawa, S., Suzuki, T., Taguchi, F., Tashiro, M., Takemori, T., Miyamura, T. & Tsunetsugu-Yokota, Y. (2006) *Virology* in press.
41. Weingartl, H., Czub, M., Czub, S., Neufeld, J., Marszal, P., Gren, J., Smith, G., Jones, S., Proulx, R., Deschambault, Y., Grudeski, E., Andonov, A., He, R., Li, Y., Copps, J., Grolla, A., Dick, D., Berry, J., Ganske, S., Manning, L. & Cao, J. (2004) *J Virol* 78, 12672-6.
42. Czub, M., Weingartl, H., Czub, S., He, R. & Cao, J. (2005) *Vaccine* 23, 2273-9.
43. Faber, M., Lamirande, E. W., Roberts, A., Rice, A. B., Koprowski, H., Dietzschold, B. & Schnell, M. J. (2005) *J Gen Virol* 86, 1435-40.
44. Wang, S., Chou, T. H., Sakhatskyy, P. V., Huang, S., Lawrence, J. M., Cao, H., Huang, X. & Lu, S. (2005) *J Virol* 79, 1906-10.
45. Kim, T. W., Lee, J. H., Hung, C. F., Peng, S., Roden, R., Wang, M. C., Viscidi, R., Tsai, Y. C., He, L., Chen, P. J., Boyd, D. A. & Wu, T. C. (2004) *J Virol* 78, 4638-45.
46. Zhu, M. S., Pan, Y., Chen, H. Q., Shen, Y., Wang, X. C., Sun, Y. J. & Tao, K. H. (2004) *Immunol Lett* 92, 237-43.
47. Zhao, P., Cao, J., Zhao, L. J., Qin, Z. L., Ke, J. S., Pan, W., Ren, H., Yu, J. G. & Qi, Z. T. (2005) *Virology* 331, 128-35.
48. Jin, H., Xiao, C., Chen, Z., Kang, Y., Ma, Y., Zhu, K., Xie, Q., Tu, Y., Yu, Y. & Wang, B. (2005) *Biochem Biophys Res Commun* 328, 979-86.
49. Okada, M., Takemoto, Y., Okuno, Y., Hashimoto, S., Yoshida, S., Fukunaga, Y., Tanaka, T., Kita, Y., Kuwayama, S., Muraki, Y., Kanamaru, N., Takai, H., Okada, C., Sakaguchi, Y., Furukawa, I., Yamada, K., Matsumoto, M., Kase, T., Demello, D. E., Peiris, J. S., Chen, P. J., Yamamoto, N., Yoshinaka, Y., Nomura, T., Ishida, I., Morikawa, S., Tashiro, M. & Sakatani, M. (2005) *Vaccine* 23, 2269-72.

Available online at www.sciencedirect.com
SCIENCE DIRECT
Virology 351 (2006) 368–380
VIROLOGY
www.elsevier.com/locate/yviro

Induction of protective immunity against severe acute respiratory syndrome coronavirus (SARS-CoV) infection using highly attenuated recombinant vaccinia virus DIs

Koji Ishii[a], Hideki Hasegawa[b], Noriyo Nagata[b], Tetsuya Mizutani[c], Shigeru Morikawa[c], Tetsuro Suzuki[a], Fumihiro Taguchi[d], Masato Tashiro[d], Toshitada Takemori[e], Tatsuo Miyamura[a], Yasuko Tsunetsugu-Yokota[e,*]

[a] *Department of Virology II, National Institute of Infectious Diseases, Toyama, Shinjuku-ku, Tokyo 162-8640, Japan*
[b] *Department of Pathology, National Institute of Infectious Diseases, Gakuen, Musashimurayama-shi, Tokyo 208-001, Japan*
[c] *Department of Virology I, National Institute of Infectious Diseases, Gakuen, Musashimurayama-shi, Tokyo 208-001, Japan*
[d] *Department of Virology III, National Institute of Infectious Diseases, Gakuen, Musashimurayama-shi, Tokyo 208-001, Japan*
[e] *Department of Immunology, National Institute of Infectious Diseases, Toyama, Shinjuku-ku, Tokyo 162-8640, Japan*

Received 22 December 2005; returned to author for revision 9 March 2006; accepted 10 March 2006
Available online 6 May 2006

Abstract

SARS-coronavirus (SARS-CoV) has recently been identified as the causative agent of SARS. We constructed a series of recombinant DIs (rDIs), a highly attenuated vaccinia strain, expressing a gene encoding four structural proteins (E, M, N and S) of SARS-CoV individually or simultaneously. These rDIs elicited SARS-CoV-specific serum IgG antibody and T-cell responses in vaccinated mice following intranasal or subcutaneous administration. Mice that were subcutaneously vaccinated with rDIs expressing S protein with or without other structural proteins induced a high level of serum neutralizing IgG antibodies and demonstrated marked protective immunity against SARS-CoV challenge in the absence of a mucosal IgA response. These results indicate that the potent immune response elicited by subcutaneous injection of rDIs containing S is able to control mucosal infection by SARS-CoV. Thus, replication-deficient DIs constructs hold promise for the development of a safe and potent SARS vaccine.

Keywords: Vaccinia virus; Vaccine; SARS

Introduction

Severe acute respiratory syndrome (SARS) has become a priority for healthcare agencies around the world given its communicability, associated mortality, and the potential for pandemic spread. As of 31 July 2003, 8,098 SARS cases had been identified worldwide, resulting in 774 deaths and a mortality rate of about 9.6% (World Health Organization statistics). SARS is now known to result from infection with a novel coronavirus (SARS-CoV) (Drosten et al., 2003; Ksiazek et al., 2003; Peiris et al., 2003). Evidence that SARS-CoV is the etiologic agent of SARS follows an experimental infection of macaques (*Macaca fascicularis*), fulfilling Koch's postulates (Fouchier et al., 2003). The clinical manifestations of SARS are hardly distinct from other common respiratory viral infections, including influenza. Because influenza epidemics might occur simultaneously with the eventual re-emergence of SARS, an effective SARS vaccine is urgently required, as well as more sensitive diagnostic tests specific for SARS.

Structural characterization of SARS-CoV and characterization of its complete RNA genome (Marra et al., 2003; Rota et al., 2003; Ruan et al., 2003) have provided us with the opportunity to develop a SARS vaccine. Like other coronaviruses, SARS-CoV is a plus-stranded RNA virus with a 30-kb genome encoding replicase gene products and the 4 structural proteins; i.e., spike (S), envelope (E), membrane (M), and nucleocapsid

* Corresponding author. Fax: +81 3 5285 1150.
E-mail address: yyokota@nih.go.jp (Y. Tsunetsugu-Yokota).

0042-6822/$ - see front matter © 2006 Elsevier Inc. All rights reserved.
doi:10.1016/j.virol.2006.03.020

(N) (Marra et al., 2003; Rota et al., 2003). The S protein is thought to be involved in receptor binding, while the E protein has a role in viral assembly, the M protein is important for virus budding, and the N protein has a role in viral RNA packaging (for review, see reference (Holmes, 2003)). Recently, angiotensin-converting enzyme 2 (ACE2) has been identified as a cellular receptor for SARS-CoV (Li et al., 2003). Thus, the first step of infection likely involves binding of S protein to the ACE2 receptor. In a model of MHV infection, S protein is known to contain important virus-neutralizing epitopes that elicit neutralizing antibody responses in mice (Collins et al., 1982). Therefore, the S protein of coronavirus might be manipulated to induce immunity. However, S, M, and N proteins are also known to contribute to the host immune response (Anton et al., 1996; Jackwood and Hilt, 1995). A DNA vaccine encoding the S glycoprotein of the SARS-CoV induces T cell and neutralizing antibody responses, as well as protective immunity, in a mouse model (Yang et al., 2004). Vaccination with a plasmid expressing N protein is capable of generating strong N-specific humoral and T-cell-mediated immune responses in vaccinated C57BL/6 mice (Kim et al., 2004; Zhao et al., 2005; Zhu et al., 2004). In addition, N-specific $CD8^+$ T cells provide protective immunity against some coronaviruses (Collisson et al., 2000; Seo et al., 1997).

The DIs strain is a highly restricted host range mutant of the vaccinia virus isolated by successive 1-day egg passage of the DIE vaccinia strain, an authorized strain for smallpox vaccine and actually used in Japan until 1981. DIs does not replicate and is not pathogenic in mice, guinea pigs or rabbits. Furthermore, the DIs does not replicate in various mammalian cell lines (Tagaya et al., 1961). Recently, we established a system for foreign gene expression by inserting target genes into this strain, after which expression of (i) bacteriophage T7 polymerase, and (ii) the full-length HIV-1_{NL432} *gag* gene, was observed (Ishii et al., 2002), thus demonstrating the usefulness of this system.

In the present study, we constructed a recombinant vaccinia virus DIs expressing one or more SARS-CoV structural proteins (E, M, N, and S, or a combination of E, M, and S (E/M/S), or E, M, N and S (E/M/N/S)). These rDIs vaccines were administered to mice either subcutaneously or intranasally, and the humoral and cellular immunity against SARS-CoV in vaccinated mice were analyzed. We demonstrated here that replication-deficient DIs constructs expressing S protein alone or in combination with other components, but not N alone, elicited strong protective immune responses against SARS-CoV infection.

Results

Expression of SARS-CoV structural proteins by rDIs

The structures of transfer vectors used in this study (pDIsSARS-E, pDIsSARS-M, pDIsSARS-N, pDIsSARS-S, pDIsSARS-E/M, pDIsSARS-E/M/S and pDIsSARS-E/M/N/S) were summarized in Fig. 1. Expression of SARS-CoV N and S proteins in chick embryo fibroblast (CEF) cells infected

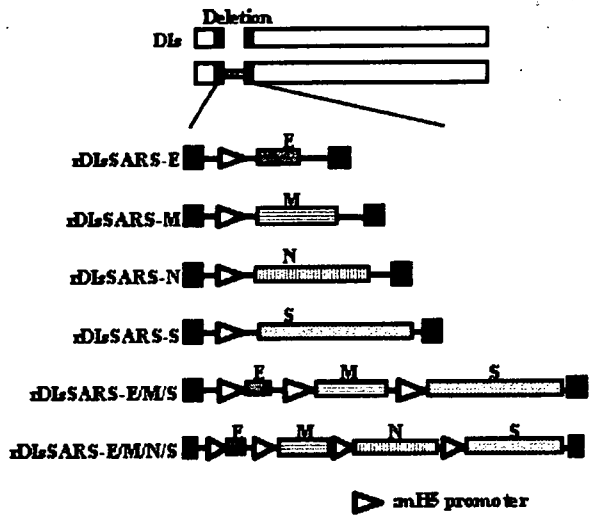

Fig. 1. Schematic diagram of rDIs constructs expressing SARS-CoV structural proteins. DNA fragments encoding E, M, N and S proteins were inserted into the location of the 15.4 kb deletion in DIs using the vaccinia virus transfer vector pDIsgptmH5. Six rDIs constructs are shown.

with rDIsSARS was detected by Western blotting using monoclonal antibodies (Fig. 2A) (Ohnishi et al., 2005). Purified SARS-CoV virion was used as a positive control (Fig. 2A, lane PC). A robust signal was detected at 50 kDa, corresponding to the N protein of SARS-CoV, as predicted by its genomic size (Marra et al., 2003; Rota et al., 2003). A band approaching 200 kDa likely corresponds to the S protein, which is known to be heavily glycosylated (Fig. 2A). Our results are consistent with data reported by Xiao et al. (2003) who expressed the full-length S glycoprotein of SARS-CoV Tor2 strain in 293 cells and demonstrated a protein approaching 180–200 kDa by SDS gel electrophoresis. Concerning the M protein, only a smear band in the stacking gel was detected using a polyclonal antibody against synthetic peptide of the M protein (Mizutani et al., 2004), presumably because it formed large oligomers with SDS-resistance in cells (Fig. 2A). Similar result was mentioned by the analysis of the M protein of SARS-CoV (Buchholz et al., 2004) and infectious bronchitis virus (Weisz et al., 1993).

The subcellular localization of S, M, and N proteins was analyzed by immunofluorescence staining. Cells infected with rDIsSARS-M demonstrated M proteins primarily co-localized with the Golgi marker GM-130 (Fig. 2B), which is consistent with the results of the recent study (Nal et al., 2005). Individually expressed SARS-CoV N protein could be detected partially with Golgi apparatus, but remained principally localized to the cytoplasm (Fig. 2B). Overexpressed recombinant SARS-S glycoprotein could be detected partially with Golgi apparatus, but also be detected throughout the cytoplasm (Fig. 2B). These results indicate that cells infected with rDIsSARS expressed significant levels of SARS-CoV proteins under the control of mH5 promoter with an expected post-translational processing (Nal et al., 2005; You et al., 2005).

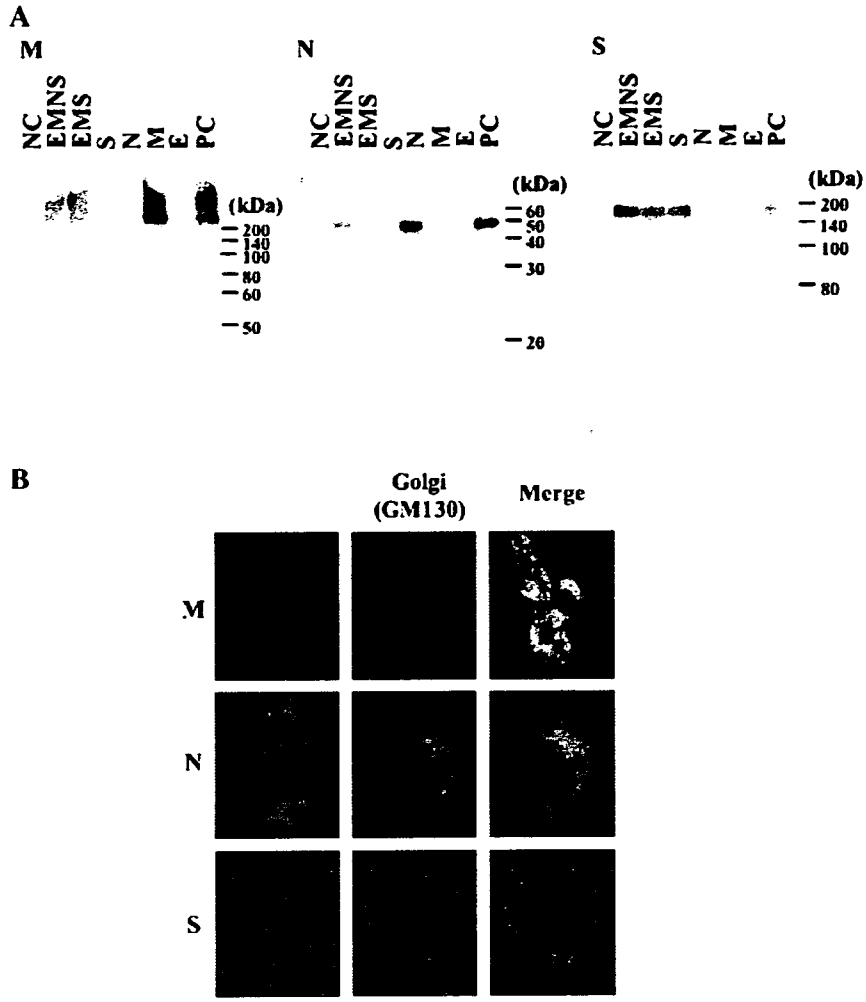

Fig. 2. Western blot analysis and indirect immunofluorescence analysis. (A) CEF cells were infected with rDIs constructs expressing SARS-CoV structural proteins (M, N and S, respectively). Purified SARS-CoV virion (0.5 μg) was used as a positive control. SARS-CoV proteins were detected using monoclonal antibodies (N and S) or polyclonal antibodies (M). Detection of bound antibodies was done with horseradish peroxidase-conjugated goat anti-mouse or anti-rabbit antibody, and visualized by chemiluminescence. (B) CEF cells were infected with rDIs constructs expressing SARS-CoV structural proteins (M, N and S, respectively). To detect SARS-CoV proteins, the cells were incubated with rabbit polyclonal antibodies against these proteins. The cells were further incubated with FITC-conjugated goat anti-rabbit IgG. To analyze subcellular localization of these proteins, monoclonal antibody against GM-130 (Golgi marker) and rhodamine-conjugated goat anti-mouse IgG were used. SARS proteins are shown in green, Golgi apparatus is shown in red and co-localization, where it occurs, is shown in yellow.

rDIsSARS induces serum IgG antibody responses specific for SARS-CoV

To examine the anti-SARS-CoV response in mice after inoculation with rDIsSARS, four mice in each group were subcutaneously or intranasally inoculated three times with 10 pfu of rDIsSARS-N, rDIsSARS-M, rDIsSARS-S, rDIs-SARS-E/M/S or rDIsSARS-E/M/N/S. Ten days after the final inoculation, vaccinated mice were observed to have high levels of anti-SARS-CoV IgG antibodies in their sera (Fig. 3).

In order to prove effective vaccination, we next examined whether neutralizing antibodies against SARS-CoV were elicited in these mice. Neutralizing antibodies against SARS-CoV were induced in mice following subcutaneous or intranasal injection of rDIsSARS-S, rDIsSARS-E/M/S, or rDIsSARS-E/M/N/S, but not in mice immunized with rDIsSARS-N or rDIsSARS-M. These results of ELISA data were incorporated into Fig. 3 by depicting the neutralization positive serum as closed circles. Thus, our results, consistent with others (Bisht et al., 2004; Buchholz et al., 2004; Yang et al., 2004), indicate that the S protein is a prerequisite for eliciting a sufficient IgG antibody response for neutralization. Similar neutralizing activity was obtained in mice receiving S alone or in combination with other components. Therefore, we expected that the rDIsSARS expressing E/M/N/S proteins in combination could be the best vaccine candidate among others.

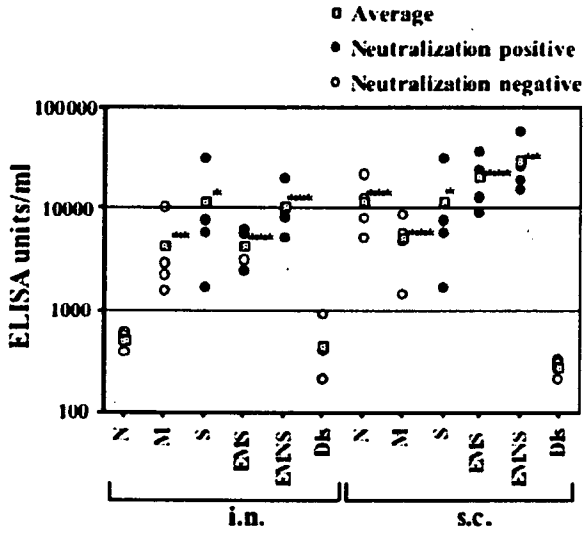

Fig. 3. Detection of anti-SARS-CoV IgG in vaccinated mice. IgG antibody levels against SARS-CoV were determined as described in Materials and methods. SARS-CoV-specific IgG titers were calculated as follows: SARS-specific IgG titer (ELISA units/ml) = (the unit value obtained for wells coated with virus-infected cell lysate) − (the unit value obtained for wells coated with non-infected cell lysate). *$P < 0.1$, **$P < 0.05$, ***$P < 0.01$ vs. DIs-administered group. The data for neutralizing sera are represented by closed circles and the data for non-neutralizing sera are represented by open circles.

Intranasal inoculation of rDIsSARS expressing E/M/N/S induces SARS-CoV-specific IgA in nasal mucosa and a high level of mucosal IgG in parallel with that of serum IgG

Mucosal IgA response is believed to be crucial for the protective immunity against various pathogens (Meeusen et al., 2004). We, next, examined mucosal immunity in the respiratory tracts of mice inoculated with rDIsSARS either subcutaneously or intranasally. The level of anti-SARS-CoV IgA within nasal wash fluid of vaccinated mice was determined by enzyme-linked immunosorbent assay (ELISA). As shown in Fig. 4A, substantial levels of anti-SARS-CoV IgA were detected only in mice received intranasal inoculation of rDIsSARS-E/M/N/S, compared to those inoculated with parental DIs ($P = 0.0010$). The level of IgA detected in intranasally rDIsSARS-E/M/N/S-inoculated mice was similar to that observed following intranasal immunization with UV-inactivated, purified SARS-CoV virion (positive control). On the other hand, subcutaneous injection of all forms of rDIsSARS produced only slightly higher levels of IgA than those observed in DIs -injected control mice. Therefore, the results indicated that the subcutaneous route of injection is inefficient, especially when mucosal IgA response is required.

Since neutralizing activity was, nevertheless, detected in the nasal washes of mice following subcutaneous immunization (data not shown), we also measured anti-SARS-CoV IgG levels in the nasal washes of these mice (Fig. 4B). High levels of IgG were detected in the nasal washes of mice following nasal immunization, which were observed to correspond well with IgG levels in the serum (Fig. 4C). A similar trend was observed in mice following subcutaneous immunization, despite at a lower level than in mice immunized intranasally. These results suggest that neutralizing IgG antibodies are capable of reaching the mucosal surface if plasma levels are high enough.

Protection of rDIsSARS-immunized mice from nasal SARS-CoV challenge is achieved without mucosal IgA response

The level of protection against SARS-CoV challenge in mice following inoculation with rDIsSARS is a critical issue for the vaccine development. We inoculated three times with 10 pfu of rDIsSARS-N, rDIsSARS-E/M/S or rDIsSARS-E/M/N/S into four mice in each group either subcutaneously or intranasally. One week after final inoculation, the mice were challenged intranasally with 10^4 tissue culture 50% infectious dose ($TCID_{50}$) of SARS-CoV. The results were shown in Fig. 4D. In mice inoculated with saline, 10^3 $TCID_{50}$/ml of SARS-CoV were recovered from lung wash fluid on day 3. In contrast, titers of SARS-CoV from the lungs of mice subcutaneously immunized with rDIsSARS-E/M/S or rDIsSARS-E/M/N/S were below the limits of detection. The same was true for mice intranasally immunized with rDIsSARS-E/M/N/S, whereas the virus was recovered in mice similarly immunized with rDIsSARS-E/M/S. Taken into consideration of a relatively low or marginal level of mucosal IgA antibody in mice intranasally immunized with rDIsSARS-E/M/N/S or rDIsSARS-E/M/S, or even no IgA response by subcutaneous route as described above, it was suggested that mucosal IgG antibody, but not IgA antibody, likely contributed to the protective immunity, especially in mice simultaneously immunized with recombinant rDIsSARS-E/M/N/S.

On the other hand, titers of SARS-CoV from the lung wash fluid of mice intranasally or subcutaneously immunized with rDIsSARS-N, were similar or slightly lower than the titers of negative controls, suggesting that intranasal or subcutaneous administration of rDIsSARS-N does not protect mice from SARS-CoV challenge, which is highly reflected by the non-neutralizing nature of anti-SARS-CoV N antibodies.

Cellular immunity induced by rDIsSARS

Although now we know that the systemic neutralizing IgG antibody against SARS-CoV S protein is a major component of protective immunity, T cell responses are also important to protect hosts from various viral infection. In a previous study of coronaviruses, S protein was shown to play an important role in viral pathogenesis, as well as induction of protective immunity (Holmes, 2003). In order to assess the ability of rDIsSARS to induce SARS-CoV S-specific T cells, T cells from axillary lymph nodes (ALN), superficial cervical lymph nodes (CLN) and spleens of mice subcutaneously immunized with rDIs-SARS-S or DIs were isolated and stimulated in vitro with UV-inactivated, purified SARS-CoV virion. Culture supernatant was collected 4 days later, and the levels of interferon-γ (IFN-γ), interleukin (IL)-2, IL-4, IL-5 and tumor necrosis factor-α (TNF-α) were measured. T cells in ALN produced the greatest cytokine levels (Fig. 5, and data not shown). This is not surprising in light of the subcutaneous route of immunization.

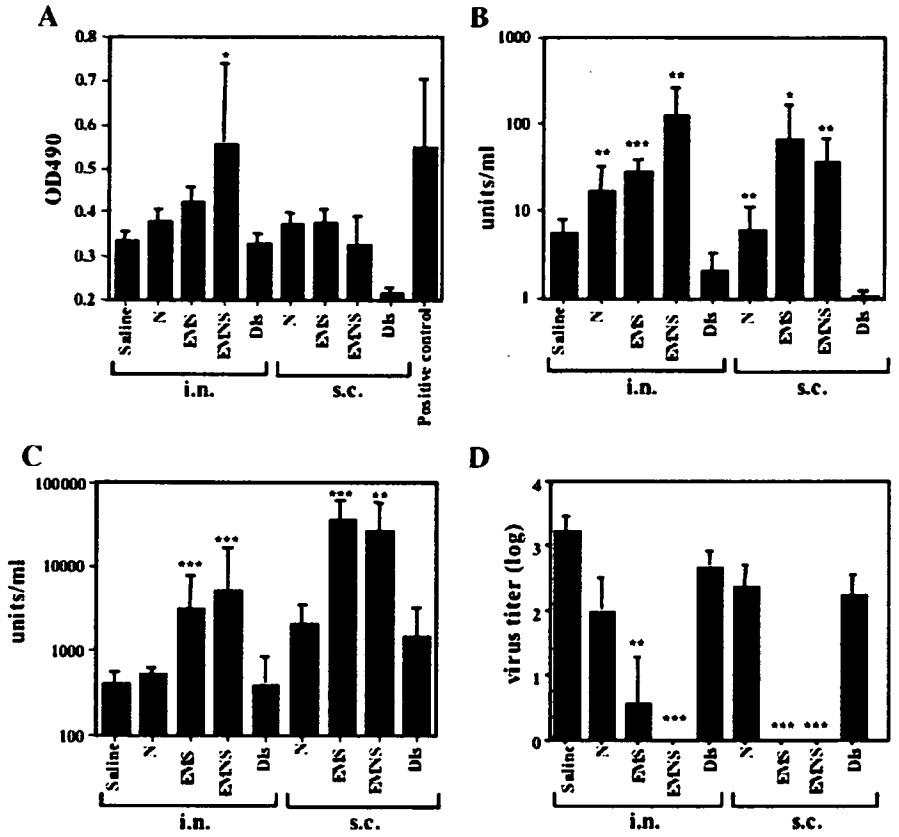

Fig. 4. Mucosally secreted anti-SARS-CoV IgG, but not IgA, antibodies are protective from nasal SARS-CoV challenge in vaccinated mice. The levels of Ig A and IgG antibodies against SARS-CoV were determined as described in Materials and methods. (A) Titers of anti-SARS-CoV IgA in the nasal washings of vaccinated mice. Error bars represent the mean ± SD. (B) Titers of anti-SARS-CoV IgG in the nasal washings of vaccinated mice. Error bars represent the mean ± SD. (C) Titers of anti-SARS-CoV IgG in the sera of vaccinated mice. Error bars represent the mean ± SD. (D) The titers of SARS-CoV in the lungs of vaccinated mice challenged 1 week later with 10^4 $TCID_{50}$ of SARS-CoV. Virus titers are expressed as $\log_{10}TCID_{50}$. Error bars represent the mean ± SD. $^*P < 0.1$, $^{**}P < 0.05$, $^{***}P < 0.01$ vs. DIs-administered group.

Notably, mice immunized with rDIsSARS-S produced a high level of IFN-γ upon in vitro stimulation with UV-inactivated, purified SARS-CoV virion. The production of TNF-α, an inflammatory cytokine, was significantly elevated in T cells in ALN of rDIsSARS-S immunized mice after in vitro stimulation with virion antigens. However, TNF-α production was observed also in mice immunized with parental DIs without in vitro stimulation with virion antigens. Since T cells from the

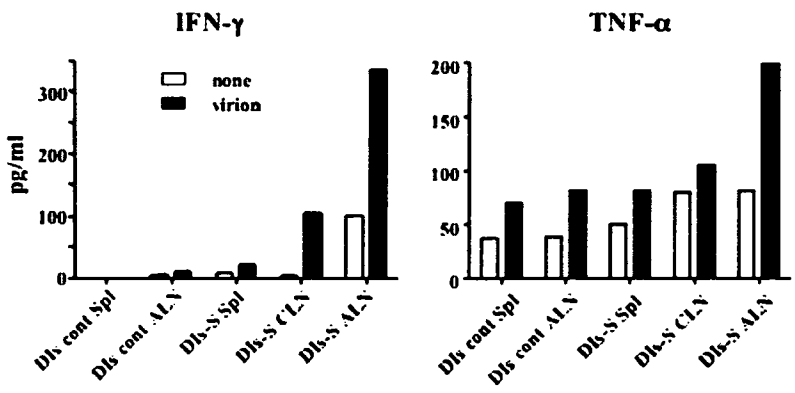

Fig. 5. In vitro response of SARS-CoV-specific T cells in mice subcutaneously immunized with rDIsSARS-S. CLN, ALN and spleens were obtained from mice 1 week after the third vaccination of either DIs control or rDIsSARS-S. After preparation of single cell suspensions, T cells were purified and cultivated with irradiated and T-cell depleted normal BALB/c mouse splenocytes as APCs in the presence or absence of 10 μg/ml of purified UV-irradiated SARS-CoV virion. Four days later, IFN-γ and TNF-α concentrations in the culture supernatant were measured.

lymph nodes of naïve mice did not produce cytokines even after in vitro stimulation with virion antigens (data not shown), it is possible that injection of DIs induces mild local inflammation, even when viral proliferation does not occur at the injection site. The pattern of IL-2, IL-5 and IL-4 production were similar to that of IFN-γ, and the maximum level of these cytokines in ALN T cells from rDIsSARS-S-immunized mice were 254, 227 and 88 ng/ml, respectively.

Next, we analyzed the antigenic epitopes of SARS-CoV-specific T cells in the spleen. We carried out IFN-γ enzyme-linked immunospot (ELISPOT) analysis using four 20-mer peptides corresponding to the ACE2 binding region of the S protein selected using the SYFPEITHI score (S44-47), as well as overlapping 20-mer peptides pool covering a whole N protein. When the splenic T cells of mice were analyzed following intranasal or subcutaneous immunization with the most potent vaccine, rDIsSARS-E/M/N/S, a high level of reactivity against S46 was observed especially in the T cells of subcutaneously immunized mice (Fig. 6A). Zhi et al. recently identified a $CD4^+$ T cell epitope, known as NYNYKYRYL, in BALB/c mice (Zhi et al., 2005). S46 contains this sequence, thus, these IFN-γ-producing T cells are likely $CD4^+$ T cells. To detect N-specific T cells, mice subcutaneously or intranasally immunized with rDIsSARS-N were analyzed by ELISPOT. In this case, ten peptides were pooled from amino-terminus of N protein, resulting in 5 pools of peptides. We thus detected N-reactive T cells capable of recognizing the first 10 peptides pool (Fig. 6B), and observed a greater proportion of N-specific T cells following nasal immunization than subcutaneous immunization. These results indicate that S- and N-specific T cells are generated systemically by rDIs.

In order to elucidate whether or not SARS-CoV-specific $CD8^+$ T cells were induced by immunization with the rDIs, the splenic T cells of mice subcutaneously or intranasally immunized with rDIsSARS-E/M/N/S were further analyzed by ELISPOT using a stably S-expressing A20.2J B cell S6.2 clone, as an antigen presenting cells (APC). Expression of S protein on the S6.2 clone was confirmed by FACS analysis using anti-SARS S monoclonal antibody (Fig. 7A). An empty vector transfectant, BOS-5, was used as a negative control APC. Subcutaneous and intranasal immunization with the most potent rDIsSARS-E/M/N/S generated a significant level of S-specific T cells (Fig. 7B), and a dramatic decrease in S-specific T cells was observed following partial depletion of $CD8^+$ T cells (Fig. 7C). Therefore, rDIsSARS-E/M/N/S was able to induce both SARS-CoV-reactive $CD4^+$ and $CD8^+$ T cells.

Histopathological findings

The immunogenicity of rDIs expressing SARS-CoV structural proteins was further evaluated by histopathological and immunohistochemical analysis of lung tissue in mice, the primary infection site of SARS-CoV (Fig. 8). Slight migration of inflammatory cells and mild disruption of the bronchial epithelium were detected in lung tissue of mock-vaccinated mice. SARS-CoV antigens were diffusely observed within the bronchial and alveolar epithelium. In contrast, significant lymphocytic infiltration into peribronchial sites, with little to no detection of SARS-CoV antigens, was observed in mice intranasally immunized with rDIsSARS-E/M/S or rDIsSARS-E/M/N/S (Fig. 8). The infiltrating lymphocytes were found to be CD3-positive T-cells, as determined by immunohistochemistry with anti-CD3 antibody (Fig. 8). On the other hand, intranasal or subcutaneous immunization by only N-expressing DIs induced neither T-cell infiltration nor protective immunity against SARS-CoV, despite of the induction of N-specific antibodies and T cells. These results suggest that marked induction of T-cell response in mice immunized with rDIsSARS-E/M/S and rDIsSARS-E/M/N/S help to eliminate SARS-CoV from the lung tissue. On the other hand, intranasal or subcutaneous immunization by only N-expressing DIs did not induce protective immunity against SARS-CoV, despite of the

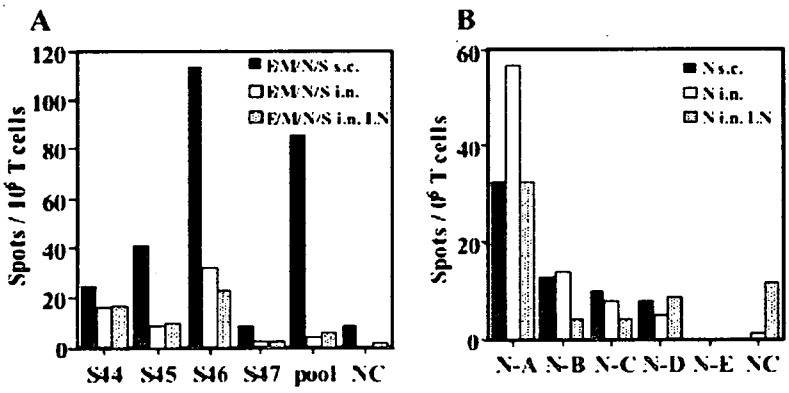

Fig. 6. Detection of SARS-CoV-specific T cells elicited by rDIsSARS-E/M/N/S or rDIsSARS-N vaccination. Splenic and lymph node (LN) T cells of mice s.c. or i.n. immunized with recombinant rDIsSARS-E/M/N/S (A) or rDIsSARS-N (B) were separated using a MACS system (Miltenyi Biotec), and IFN-γ ELISPOT analysis was performed. (A) T cells (5×10^5 cells) from mice immunized with rDIsSARS-E/M/N/S were cultured with irradiated A20.2J B cells (1×10^4), in triplicate, in a 96-well membrane plates coated with IFN-γ capture antibody in the absence or presence of 5 μM of S peptides (S44–S47). The numbers of IFN-γ spot-forming cells were then counted and are depicted. (B) T cells from mice immunized with rDIsSARS-N and A20.2J B cells were cultured as described in A. N protein (422 amino acids) was divided into 5 parts by 100 amino acids (A, B, C, D and E) and 10 peptides each of pooled 20-mer overlapping peptides specific to the each stretch of N sequence were used as an antigen.

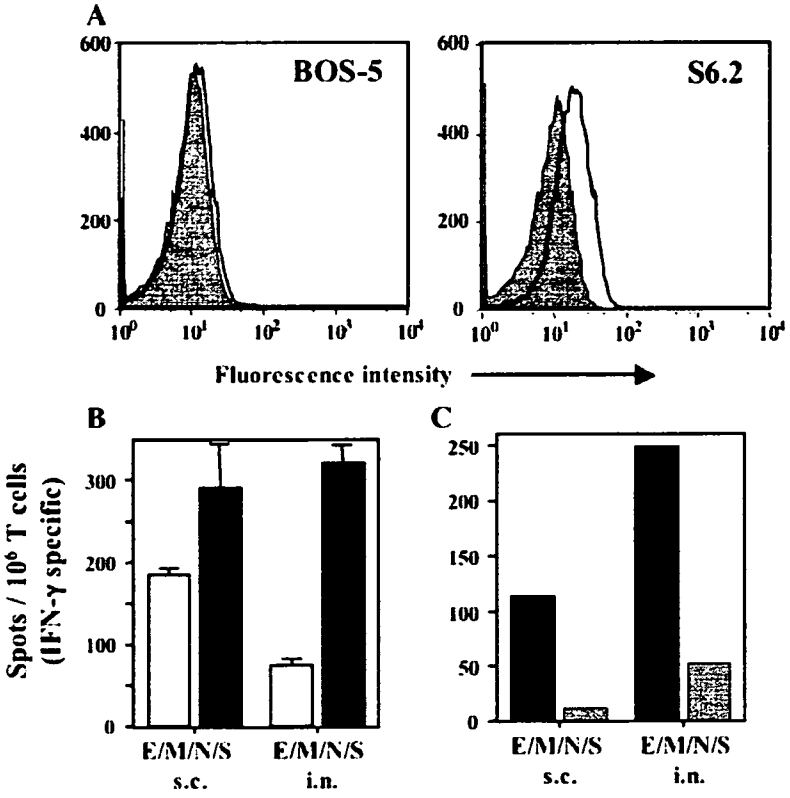

Fig. 7. Detection of SARS-CoV S-specific $CD8^+$ T cells in mice immunized with rDIsSARS-E/M/N/S. (A) A20.2J B cell clone expressing S (S6.2) or empty vector (BOS-5) was stained with biotinylated anti-SARS-CoV S monoclonal antibody (solid line) or control IgG (shadowed line), followed by the incubation with streptavidin-APC, and then analyzed by FACScalibur. A histogram of APC fluorescence of gated live cells (PI negative) is depicted. (B) Splenic T cells from mice immunized s.c. or i.n. with recombinant rDIsSARS-E/M/N/S were purified and IFN-γ ELISPOT analysis was carried out using γ-irradiated S6.2 and BOS-5 as APCs. The number of T cells reactive for BOS-5 control (white column) and S6.2 (black column) cells are shown. Error bars represent the mean ± SD. (C) Using the same splenic T cells as in panel B, $CD8^+$ T cells were partially removed using anti-CD8 mAb-coated magnetic beads (Miltenyi Biotec), and the number of T cells reactive for BOS-5 and S6.2 cells were counted by ELISPOT. The number of BOS-5-reactive T cells was subtracted and the number of S-specific T cells is depicted. Black columns: total T cells; grey columns: partially CD8-depleted T cells.

induction of N-specific antibodies and T cells. Thus, rDIs expressing the S protein, along with other membrane components (E/M and E/M/N), are capable of inducing strong immunity of both humoral and cellular arms and are fully competent to clear SARS-CoV infection.

Discussion

The DIs strain, which replicates well in CEF cells but not in most mammalian cells, was isolated from the DIE strain of the vaccinia virus during serial 1-day egg passage, and it is characterized by the induction of tiny pocks on chicken chorioallantoic membrane (Tagaya et al., 1961; Kitamura et al., 1967; Ishii et al., 2002). The DIs-derived recombinant viruses express high levels of viral and inserted genes, even in non-permissive cell lines without any cytopathic effects (Ishii et al., 2002). In earlier studies, MVA strain of vaccinia virus, which is also replication-incompetent in most mammal cells, was used to express a variety of foreign genes and some of these recombinant viruses were studied as candidate vaccine vectors and appeared to be more effective than many replication-competent vaccinia virus vaccines (Sutter and Moss, 1992; Sutter et al., 1994; Belyakov et al., 1998; Nam et al., 1999; Stittelaar et al., 2000). rDIs does not replicate nor produce infectious virions in most mammalian cells, therefore the DIs strain has a safety advantage when used as a recombinant vaccine vector as for MVA. Recently, a recombinant DIs, rDIsSIVGag, expressing a full-length *gag* gene of SIV, was developed, and demonstrated to have a potential for use as an HIV/AIDS vaccine (Someya et al., 2004).

Attempts at vaccine development against SARS-CoV are ongoing by a number of organizations using various techniques (see review, (Groneberg et al., 2005)). DNA vaccines (Kim et al., 2004; Yang et al., 2004; Zhu et al., 2004; Zhao et al., 2005) and viral vectors such as vaccinia virus (Bisht et al., 2004; Weingartl et al., 2004), parainfluenza virus (Bukreyev et al., 2004), adenovirus (Zakhartchouk et al., 2005) and rhabdoviruses (Faber et al., 2005; Kapadia et al., 2005) are used as recombinant vaccines. Yang et al. (2004) showed that viral replication was reduced by more than six orders of magnitude in the lungs of mice vaccinated with these S plasmid DNA expression vectors, and protection was mediated by a humoral but not a T-cell-dependent immune mechanism. Bisht et al. (2004) showed that inoculation of BALB/c mice with a

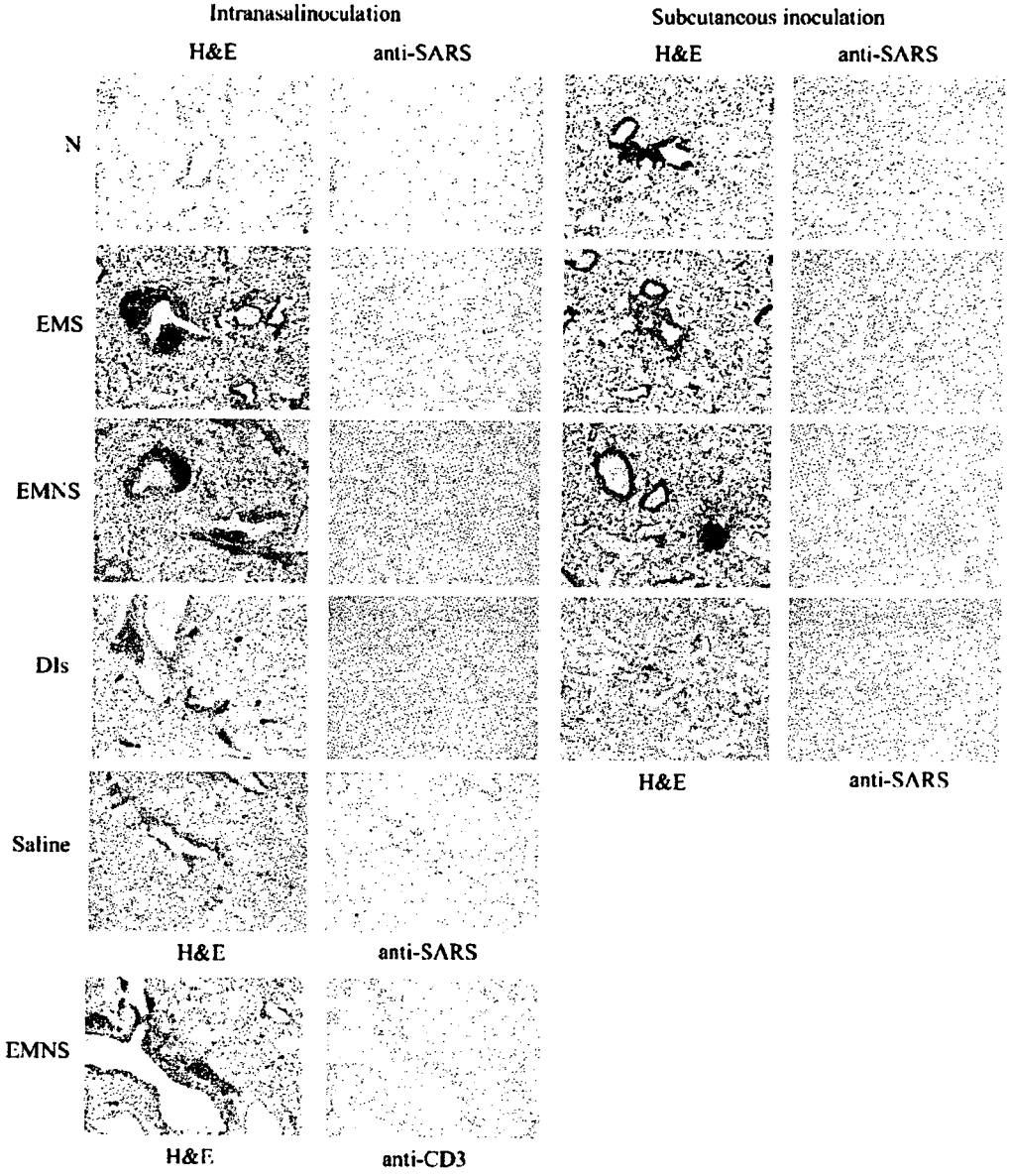

Fig. 8. Histopathology and immunohistochemistry. Lung specimen of mice immunized with rDIs expressing structural proteins of SARS-CoV and challenged with SARS-CoV. Mice were immunized i.n. or s.c. with DIs, rDIsSARS-N, rDIsSARS-E/M/S, rDIsSARS-E/M/N/S or saline. Mice were challenged with SARS-CoV 2 weeks after the final vaccination. Lungs were harvested 3 days after the challenge. The section was stained with hematoxylin and eosin (H&E) or immunohistochmically stained with anti-SARS-CoV antibody or anti-CD3 antibody.

recombinant MVA expressing SARS-CoV S protein elicited serum antibodies to SARS-CoV S protein and protective immunity against SARS-CoV infection. Previous studies demonstrated passive transfer of serum from immunized mice conferred protection against SARS-CoV in the respiratory tract following inoculation with either SARS CoV or recombinant MVA expressing S protein (Bisht et al., 2004; Subbarao et al., 2004). These results suggest that S protein is a crucial antigen in generating protective immunity. We observed that intranasal or subcutaneous inoculation of BALB/c mice with rDIs expressing S protein (rDIsSARS-S, rDIsSARS-E/M/S or rDIsSARS-E/M/N/S) produced serum antibodies capable of recognizing the SARS-CoV virion by ELISA, also capable of neutralizing SARS-CoV in vitro. The subcutaneous route appears to elicit stronger immunity than intranasal immunization with respect to the level of anti-SARS-CoV IgG antibody produced. Important finding here is that although the mucosal IgA antibody response was induced only in mice intranasally immunized with rDIsSARS-E/M/N/S, the mice administered with rDIsSARS-E/M/N/S by either route elicited strong protective immunity. Therefore, the protection was achieved in the absence of a mucosal IgA response in mice subcutaneously immunized with rDIsSARS-E/M/N/S. Thus, our results clearly show that mucosal infection might be prevented in the presence of a

high level of neutralizing serum IgG antibody. Control mice vaccinated with DIs not expressing envelope proteins were not protected, indicating that the effect was specific for the expressed envelope proteins of SARS-CoV and was not due to enhanced nonspecific immunity.

A recent report suggests that a combination of three adenovirus vector expressing SARS-S, -M and –N protein is capable of eliciting neutralizing antibodies in serum and N-specific T cell responses in rhesus macaques (Gao et al., 2003). However, in this report, the relationship between these immune responses and actual protection was not presented. In another study, the importance of SARS-CoV structural proteins in generating protective immunity was investigated by expressing them individually and in combination using a recombinant parainfluenza virus (PIV) type 3 vector. The expression of S with the two other putative virion envelope proteins, M and E protein, did not augment the neutralizing antibody response. In the absence of S, expression of M and E, or the nucleocapsid protein N, did not induce a detectable serum SARS-CoV-neutralizing antibody response (Buchholz et al., 2004). Our results were consistent with this in that expression of M or N proteins by administration of DIs harboring SARS-CoV M or N gene singly did not induce a neutralizing antibody response, although anti-SARS-CoV antibodies were detected by ELISA.

Recent studies have shown that vaccination with a plasmid expressing N protein can elicit SARS-CoV nucleocapsid-specific humoral and cellular immune responses (Kim et al., 2004; Zhu et al., 2004; Zhao et al., 2005). They showed that linkage of N protein to calreticulin, Ca^{2+}-binding protein known to enhance immune response, in a DNA vaccine resulted in the significant enhancement of the humoral and cellular immune responses to N protein in vaccinated mice. They also showed that the N protein-specific DNA vaccine elicited partial protection against N protein expressing vaccinia virus challenge, however, the efficacy of N-specific cellular immune responses in protection of SARS-CoV infection is not clear. Although we here showed that N protein expression by rDIs was capable of eliciting N-specific humoral and cellular immunity, vaccination with rDIsSARS-N failed to elicit a neutralizing antibody response against SARS-CoV infection in vitro, and failed to confer full protection in vaccinated mice against SARS-CoV challenge, suggesting that SARS-CoV N protein-specific antibodies and CTLs were not sufficient to provide full protection against SARS-CoV infection.

Histopathological analysis of lung tissues in the present study revealed a marked lymphocytic infiltration in peribronchial sites in mice immunized intranasally or subcutaneously with recombinant vaccinia virus DIs expressing E/M/S or E/M/N/S. Almost no SARS-CoV antigens were detected in these areas upon immunohistochemical analysis. The infiltrating lymphocytes were shown to be CD3 positive T-cells. This is the first evidence of induction of protective immunity against SARS-CoV associated with marked infiltration of T cells at a SARS-CoV infection site. We were able to detect SARS-CoV S-specific $CD8^+$ T cells in the spleen of these immunized mice by INF-γ ELISPOT. Thus, these results suggest that T cell induction in mice immunized with rDIsSARS-E/M/S and rDIsSARS-E/M/N/S might provide additional help to completely eliminate SARS-CoV in the lung. Of note, Weingartl et al. (2004) reported a low level of neutralizing antibody response in ferrets (*Mustela putorius furo*) immunized with a recombinant MVA expressing SARS-CoV S protein. They also showed that there are more rapid and vigorous neutralizing antibody responses in immunized ferrets, compared to control animals after challenge with SARS-CoV. However, SARS-CoV infection and spreading in the immunized ferrets is not prevented. Moreover, upon infection with SARS-CoV, strong inflammatory responses were noted in ferrets immunized with either recombinant MVA expressing SARS-CoV S or N protein, suggesting that vaccination with the recombinant MVA expressing SARS-CoV S or N protein may, in some case, lead to enhanced pathology during SARS-CoV infection (Czub et al., 2005; Weingartl et al., 2004). It was also reported that antibodies that neutralized most human SARS-CoV S enhanced entry mediated by the civet virus S, suggesting the possibility that such kind of vaccines might enhance viral infection (Yang et al., 2005). Although we observed no such pathology in rDIs-immunized mice after virus challenge, the potential for widespread tissue damage following administration of SARS-CoV proteins should be carefully investigated. In addition, further studies are required to clarify whether the recruited T-cells indeed play an important role in clearance of SARS-CoV from sites of infection.

In this study, we constructed rDIs containing genes encoding four structural proteins of SARS-CoV that were individually or simultaneously expressed. Intranasal or subcutaneous inoculation of BALB/c 3T3 mice with rDIs expressing S protein with or without other structural proteins elicited a high level of neutralizing antibodies against SARS-CoV and protective immunity, in the lungs of mice after intranasal challenge. Furthermore, both cellular and mucosal immunity against SARS-CoV structural proteins were also induced following administration of the rDIs. Therefore, the replication-deficient DIs strain is a feasible, safe and effective SARS vaccine vector.

Materials and methods

Cells

CEF cells and Vero E6 cells were grown in Dulbecco's modified essential medium (DMEM) supplemented with 10% fetal bovine serum (FCS), 1% penicillin-streptomycin and L-glutamine (GIBCO BRL/Life Technologies, Gaithersburg, MD). A20.2J murine B cells were maintained in RPMI1640 supplemented with 10% FCS, 50 μM β-mercaptoethanol, L-glutamine and antibiotics.

Plasmid DNA constructs and DNA preparation

cDNA encoding SARS-CoV structural proteins were generated by reverse transcription of SARS-CoV HKU39849

(Accession No. AY278491) using superscriptII (Invitrogen Corp., Carlsbad, CA), followed by amplification using expand high fidelity PCR system (Roche diagnostics), as described previously (Ohnishi et al., 2005). These DNA fragments encoding E, M, N and S proteins were cloned into the vaccinia virus transfer vector pDIsgptmH5, which also harbored E. coli xanthine-guanine phosphoribosyltransferase, under control of a vaccinia virus p7.5 promoter in the cloning site of pUc/DIs (Ishii et al., 2002), to generate pDIsSARS-E, pDIsSARS-M, pDIsSARS-N, and pDIsSARS-S, respectively. To construct transfer vectors to generate rDIs expressing E/M, E/M/S, or E/M/N/S, DNA fragments encoding M, N and S proteins controlled by the mH5 promoter of the vaccinia virus (Wyatt et al., 1996) were inserted into pDIsSARS-E *Sma*I, *Not*I and *Sac*I sites, respectively, thus generating pDIsSARS-E/M, pDIsSARS-E/M/S and pDIsSARS-E/M/N/S (Fig. 1). A plasmid expressing S driven by the EF-1α promoter was constructed using pEF-BOS-bst (Yoshizawa et al., 2001), and designated pEF-S-bst.

Generation of recombinant vaccinia virus

Recombinant forms of DIs were obtained by hypoxanthine-guanine phosphoribosyltransferase selection (Falkner and Moss, 1988). Monolayers of CEF cells in 6-well plates were pre-incubated with DMEM containing 10% FCS, 25 μg/ml of micophenoic acid (MPA), 250 μg/ml of xanthine and 15 μg/ml of hypoxanthine. Infection was performed onto CEF cells grown in 8 cm dishes with DIs at a multiplicity of infection (moi) of 1.0. Transfection was performed using 20 μg of each DIs transfer vector and Lipofectamine (GIBCO BRL/Life Technologies). rDIs expressing SARS-CoV structural proteins were selected following four consecutive rounds of plaque purification of CEF cells in 6-well plates pre-incubated with DMEM containing 10% FCS, 25 μg/ml of MPA, 250 μg/ml of xanthine, and 15 μg/ml of hypoxanthine. Resultant rDIs expressing SARS-CoV structural proteins were designated as rDIsSARS-E, rDIsSARS-M, rDIsSARS-N, rDIsSARS-S, rDIsSARS-E/M, rDIsSARS-E/M/S and rDIsSARS-E/M/N/S, respectively, and subsequently maintained in CEF cells for use in further studies.

Western blot analysis

CEF cells infected with rDIs constructs harboring ORFs of SARS-CoV structural proteins were fractionated by SDS-PAGE under reduced conditions. Purified SARS-CoV virion (0.5 μg) was used as a positive control. The proteins were then transferred to an Immobilon-P PVDF membrane (MILLIPORE, Bedford, MA) and incubated with monoclonal antibodies against N or S proteins (Ohnishi et al., 2005) or polyclonal antibody against M protein (Mizutani et al., 2004). After washing, the membrane was reacted with HRP-conjugated Fab fragment of anti-mouse or rabbit IgG (H + L) (1:20,000, Santa Cruz Biotechnology, Santa Cruz, CA), followed by visualization of the bands using chemiluminescent reagents (Pierce, Rockford, IL).

Indirect immunofluorescence analysis

CEF cells were infected with rDIs expressing SARS-CoV structural proteins. After 48 h of incubation, the cells were washed with PBS and fixed with 3% paraformaldehyde in PBS for 20 min at room temperature. The fixed cells were then permeabilized with 0.2% Triton X-100 for 3 min at room temperature, and then blocked with a non-fat milk solution, Block Ace (Yukijirushi Co., Tokyo, Japan). The cells were incubated with polyclonal antibodies against M, N or S proteins (Mizutani et al., 2004) for 60 min at 37 °C. The cells were further incubated with fluorescein isothiocyanate (FITC)-conjugated goat anti-rabbit IgG (TAGO, Burlingame, CA) diluted to 1:500 in PBS to detect SARS-CoV M, N or S proteins. To analyze the subcellular localization of SARS structural proteins, anti-GM-130 monoclonal antibody (BD Biosciences, Mississauga, ON, Canada) and rhodamine-conjugated goat anti-mouse IgG (TAGO) were used to stain the Golgi apparatus.

Vaccination

Animal studies were carried out under a protocol approved by the Animal Care and Use Committee of the National Institute of Infectious Diseases, Japan. Five- to 6-week-old female BALB/c mice were purchased from Japan SLC (Hamamatsu, Japan) and immunized with 10^6 pfu of rDIs, either subcutaneously (s.c.) or intranasally (i.n.). After 2 and 6 weeks, identical titers of recombinant virus were re-administered. One week later, the mice were intranasally challenged with 10^4 $TCID_{50}$ of SARS-CoV in 20 μl of saline as previously described (Subbarao et al., 2004). Three days later, serum, nasal wash fluid and bronchoalveolar wash fluid were collected to measure viral titers and antibodies against SARS-CoV from mice that were sacrificed under anesthesia with chloroform.

Detection of SARS-CoV specific IgA and IgG antibodies

IgA and IgG titers against SARS-CoV were determined by ELISA, as previously described (Takasuka et al., 2004). Briefly, microtiter plates (Dynatech, Chantily, VA) were coated overnight at 4 °C with SARS-CoV-infected or mock-infected Vero E6 cell lysate samples previously treated with 1% NP40, followed by UV-inactivation. The plates were blocked with 1% OVA in PBS–0.05% Tween 20, and then incubated with serially diluted sera (1:10–$1:25^5$) for 1 h at room temperature. The plates were then incubated with either peroxidase-conjugated anti-mouse IgG (1:2000, Zymed, South San Francisco, CA) or IgA (1:2000, Southern Biotechnology, Birmingham, AL) antibody. The plates were washed three times with PBS-Tween at each step. The substrate mixture (o-phenylenediamine (Zymed) and hydrogen peroxide) was added to each well, and the absorbance of each well was read at 490 nm using a model 680 microplate reader (Bio-Rad, Hercules, CA). To provide a standard for IgG detection, serum was obtained from a hyper-immunized mouse and the OD490nm value of 100 ELISA units/ml of standard serum was around three in every assay.

Each SARS-CoV-specific IgG titer was calculated by subtracting the optical density of wells coated with non-infected cell lysate from the optical density of wells coated with virus-infected cell lysate. As a positive control to induce SARS-CoV-specific IgA, mice were immunized intranasally with UV-inactivated purified SARS-CoV together with 3 μg of poly(I:C) (Ichinohe et al., 2005).

SARS-CoV neutralizing assay

Sera collected from vaccinated mice were inactivated by incubation at 56 °C for 30 min. The serially diluted mice sera (up to five-fold) were incubated with 100 $TCID_{50}$ of SARS-CoV for 1 h, then the mixtures were added to a Vero E6 cell culture grown to confluence in 96-well microtiter plates. After 48 h, the cells were fixed with 10% formaldehyde and stained with crystal violet to visualize the cytopathic effects of the virus (Storch, 2001). Neutralization antibody titers were expressed as the minimal dilution of sera capable of inhibiting viral cytopathic effects.

Analysis of the SARS-CoV-specific T-cell response

CLN, ALN and spleens were obtained from mice 1 week after their third vaccination. Following preparation of a single cell suspension, T cells were purified using a Pan T cell isolation kit and a magnetic cell sort system (MACS: Miltenyi Biotec, Bergisch Gladbach, Germany). To prepare APC, normal BALB/c mouse splenocytes were depleted of Thy-1^+ T cells by MACS and irradiated at 2000 cGy. Purified T cells (1×10^6) were cultured with APC (5×10^6) in the presence or absence of UV-irradiated, purified SARS-CoV virion at 10 μg/ml. Four days after cultivation, cytokine concentrations within culture supernatant were measured by flow cytometry using a mouse Th1/Th2 cytokine cytometric bead array kit (Becton Dickinson, San Jose, CA).

Generation of a stable S-transfectant

A20.2J murine B cells were transfected with either pEF-S-bst or pEF-BOS-bst by electroporation at 960 μF and 310 V using a GenePulser (BioRad Laboratories, Hercules, CA). After selection using blasticidine S (Invitrogen), followed by limiting dilution cloning, S6.2 and BOS-5 clones were obtained. To detect S protein expression in S6.2 cells, the cells were stained with biotinylated anti-S monoclonal antibody (Ohnishi et al., 2005) or control antibody, followed by the incubation with APC-streptavidin (e-Bioscience Inc., San Diego, CA), after which they were analyzed by FACScalibur (BD Bioscience) using the Cell Quest II program. Propidium Iodide was used to exclude dead cells. The data were re-analyzed and depicted using Flowjo software (Tree Star Inc., San Carlos, CA).

ELISPOT assay

Spleen T cells of mice immunized with rDIsSARS-N or rDIsSARS- E/M/N/S were separated using a MACS system (Miltenyi Biotec, Auburn, CA). To enrich $CD4^+$ T cells in the T cell fraction, $CD8^+$ T cells were partially removed using anti-CD8 mAb-coated magnetic beads (Miltenyi Biotec). This procedure reduced the number of $CD8^+$ T cells to less than one third. Overlapping 20-mer peptides covering the whole N sequences of SARS-CoV were obtained from Sigma-Aldrich Japan. S peptides S44 (S331–350), S45 (S381–400), S46 (S431–450), and S47 (S481–500) corresponding to the ACE2 binding region of the S protein were selectively produced based on a web-site program by SYFPEITHI (http://syfpeithi.de/). A20.2J murine B cells irradiated at 2000 cGy were used as APCs with peptides corresponding to either S or N proteins. In some experiments, A20.2J cells stably transfected with pEF-S or the empty vector pEF-BOS were used.

ELISPOT assays were performed according to the methods outlined by DIACLONE research (Besancon, France). In brief, 96-well flat-bottom plates (Maxisoap Nunc plates, Nunc, Rochester, NY) were coated with anti-IFN-γ capture antibody for one h at 37 °C. The plates were then washed with PBS containing 0.05% Tween 20 (PBST), and blocked with PBS containing 2% bovine serum albumin overnight at 4 °C. Freshly isolated splenic T cells (5×10^5) and APCs (1×10^4) were added to the plates in the presence or absence of 5 μM of N or S peptides and incubated for 16 h at 37 °C in 5% CO_2 on the anti-IFN-γ-coated plates, followed by a lysis with ice-cold deionized water. After the plates were washed, biotinylated detection antibody was added, then the plates were further incubated for 1 h at 37 °C. The plates were washed three times with PBST, then 50 μl/well of Streptavidin-alkaline phosphatase-conjugated anti-biotin immunoglobulin G solution was added, followed by incubation for 1 h at 37 °C. After washing with PBST, substrate mix (50 μl/well) was added, and the plates were allowed to develop over 4 h at 37 °C. The wells were imaged and the number of spot-forming cells SFC counted using a KS ELISPOT compact system (Carl Zeiss, Jena, Germany).

Histopathology and immunohistochemistry

Lung tissue from the mice was fixed in 10% buffered formalin and embedded in paraffin. Paraffin block sections were stained with hematoxylin and eosin (H&E). SARS-CoV antigens were immunohistochemically detected using a labeled-streptoavidin–biotin complex staining system (DakoCytomation Co. Japan, Kyoto, Japan). Rabbit polyclonal antibodies raised against UV-inactivated, purified SARS-CoV were used as a primary antibody. A catalyzed signal amplification method (Dako) was also used to detect SARS-CoV antigens with enhanced sensitivity. Lung sections from mice vaccinated with rDIsSARS-E/M/N/S and infected with SARS Co-V were stained with anti-CD3 antibody. (Santa Cruz Biotechnology)

Acknowledgments

We would like to thank Dr. Michinori Kohara for kindly providing us anti-SARS-CoV polyclonal antibodies. We would

also like to thank Ms. Mami Matsuda, Ms. Makiko Yahata, Ms. Sayaka Yoshizaki, Ms. Chikako Sato, Mr. Masayuki Ishige, Ms. Yuko Sato and Ms. Aya Harashima for their excellent technical support. This work was supported by a Heath and Labour Science Research Grant from the Ministry of Health, Labour, and Welfare, Japan, and from the New Energy and Industrial Technology Development Organization (NEDO) of Japan.

References

Anton, I.M., Gonzalez, S., Bullido, M.J., Corsin, M., Risco, C., Langeveld, J.P., Enjuanes, L., 1996. Cooperation between transmissible gastroenteritis coronavirus (TGEV) structural proteins in the in vitro induction of virus-specific antibodies. Virus Res. 46 (1–2), 111–124.

Belyakov, I.M., Wyatt, L.S., Ahlers, J.D., Earl, P., Pendleton, C.D., Kelsall, B.L., Strober, W., Moss, B., Berzofsky, J.A., 1998. Induction of a mucosal cytotoxic T-lymphocyte response by intrarectal immunization with a replication-deficient recombinant vaccinia virus expressing human immunodeficiency virus 89.6 envelope protein. J. Virol. 72, 8264–8272.

Bisht, H., Roberts, A., Vogel, L., Bukreyev, A., Collins, P.L., Murphy, B.R., Subbarao, K., Moss, B., 2004. Severe acute respiratory syndrome coronavirus spike protein expressed by attenuated vaccinia virus protectively immunizes mice. Proc. Natl. Acad. Sci. U. S. A. 101 (17), 6641–6646.

Buchholz, U.J., Bukreyev, A., Yang, L., Lamirande, E.W., Murphy, B.R., Subbarao, K., Collins, P.L., 2004. Contributions of the structural proteins of severe acute respiratory syndrome coronavirus to protective immunity. Proc. Natl. Acad. Sci. U. S. A. 101 (26), 9804–9809.

Bukreyev, A., Lamirande, E.W., Buchholz, U.J., Vogel, L.N., Elkins, W.R., St Claire, M., Murphy, B.R., Subbarao, K., Collins, P.L., 2004. Mucosal immunisation of African green monkeys (*Cercopithecus aethiops*) with an attenuated parainfluenza virus expressing the SARS coronavirus spike protein for the prevention of SARS. Lancet 363 (9427), 2122–2127.

Collins, A.R., Knobler, R.L., Powell, H., Buchmeier, M.J., 1982. Monoclonal antibodies to murine hepatitis virus-4 (strain JHM) define the viral glycoprotein responsible for attachment and cell–cell fusion. Virology 119 (2), 358–371.

Collisson, E.W., Pei, J., Dzielawa, J., Seo, S.H., 2000. Cytotoxic T lymphocytes are critical in the control of infectious bronchitis virus in poultry. Dev. Comp. Immunol. 24 (2–3), 187–200.

Czub, M., Weingartl, H., Czub, S., He, R., Cao, J., 2005. Evaluation of modified vaccinia virus Ankara based recombinant SARS vaccine in ferrets. Vaccine 23 (17–18), 2273–227 9.

Drosten, C., Gunther, S., Preiser, W., van der Werf, S., Brodt, H.R., Becker, S., Rabenau, H., Panning, M., Kolesnikova, L., Fouchier, R.A., Berger, A., Burguiere, A.M., Cinatl, J., Eickmann, M., Escriou, N., Grywna, K., Kramme, S., Manuguerra, J.C., Muller, S., Rickerts, V., Sturmer, M., Vieth, S., Klenk, H.D., Osterhaus, A.D., Schmitz, H., Doerr, H.W., 2003. Identification of a novel coronavirus in patients with severe acute respiratory syndrome. N. Engl. J. Med. 348 (20), 1967–1976.

Faber, M., Lamirande, E.W., Roberts, A., Rice, A.B., Koprowski, H., Dietzschold, B., Schnell, M.J., 2005. A single immunization with a rhabdovirus-based vector expressing severe acute respiratory syndrome coronavirus (SARS-CoV) S protein results in the production of high levels of SARS-CoV-neutralizing antibodies. J. Gen. Virol. 86 (Pt. 5), 1435–1440.

Falkner, F.G., Moss, B., 1988. *Escherichia coli* gpt gene provides dominant selection for vaccinia virus open reading frame expression vectors. J. Virol. 62 (6), 1849–1854.

Fouchier, R.A., Kuiken, T., Schutten, M., van Amerongen, G., van Doornum, G.J., van den Hoogen, B.G., Peiris, M., Lim, W., Stohr, K., Osterhaus, A.D., 2003. Aetiology: Koch's postulates fulfilled for SARS virus. Nature 423 (6937), 240.

Gao, W., Tamin, A., Soloff, A., D'Aiuto, L., Nwanegbo, E., Robbins, P.D., Bellini, W.J., Barratt-Boyes, S., Gambotto, A., 2003. Effects of a SARS-associated coronavirus vaccine in monkeys. Lancet 362 (9399), 1895–1896.

Groneberg, D.A., Poutanen, S.M., Low, D.E., Lode, H., Welte, T., Zabel, P., 2005. Treatment and vaccines for severe acute respiratory syndrome. Lancet, Infect. Dis. 5 (3), 147–155.

Holmes, K.V., 2003. SARS coronavirus: a new challenge for prevention and therapy. J. Clin. Invest. 111 (11), 1605–1609.

Ichinohe, T., Watanabe, I., Ito, S., Fujii, H., Moriyama, M., Tamura, S., Takahashi, H., Sawa, H., Chiba, J., Kurata, T., Sata, T., Hasegawa, H., 2005. Synthetic double-stranded RNA poly (I:C) combined with mucosal vaccine protects against influenza virus infection. J. Virol. 79 (5), 2910–2919.

Ishii, K., Ueda, Y., Matsuo, K., Matsuura, Y., Kitamura, T., Kato, K., Izumi, Y., Someya, K., Ohsu, T., Honda, M., Miyamura, T., 2002. Structural analysis of vaccinia virus DIs strain: application as a new replication-deficient viral vector. Virology 302 (2), 433–444.

Jackwood, M.W., Hilt, D.A., 1995. Production and immunogenicity of multiple antigenic peptide (MAP) constructs derived from the S1 glycoprotein of infectious bronchitis virus (IBV. Adv. Exp. Med. Biol. 380, 213–219.

Kapadia, S.U., Rose, J.K., Lamirande, E., Vogel, L., Subbarao, K., Roberts, A., 2005. Long-term protection from SARS coronavirus infection conferred by a single immunization with an attenuated VSV-based vaccine. Virology 340, 174–182.

Kim, T.W., Lee, J.H., Hung, C.F., Peng, S., Roden, R., Wang, M.C., Viscidi, R., Tsai, Y.C., He, L., Chen, P.J., Boyd, D.A., Wu, T.C., 2004. Generation and characterization of DNA vaccines targeting the nucleocapsid protein of severe acute respiratory syndrome coronavirus. J. Virol. 78 (9), 4638–4645.

Kitamura, T., Kitamura, T., Tagaya, I., 1967. Immunogenicity of an attenuated strain of vaccinia virus on rabbits and monkeys. Nature 215, 1187–1188.

Ksiazek, T.G., Erdman, D., Goldsmith, C.S., Zaki, S.R., Peret, T., Emery, S., Tong, S., Urbani, C., Comer, J.A., Lim, W., Rollin, P.E., Dowell, S.F., Ling, A.E., Humphrey, C.D., Shieh, W.J., Guarner, J., Paddock, C.D., Rota, P., Fields, B., DeRisi, J., Yang, J.Y., Cox, N., Hughes, J.M., LeDuc, J.W., Bellini, W.J., Anderson, L.J., 2003. A novel coronavirus associated with severe acute respiratory syndrome. N. Engl. J. Med. 348 (20), 1953–1966.

Li, W., Moore, M.J., Vasilieva, N., Sui, J., Wong, S.K., Berne, M.A., Somasundaran, M., Sullivan, J.L., Luzuriaga, K., Greenough, T.C., Choe, H., Farzan, M., 2003. Angiotensin-converting enzyme 2 is a functional receptor for the SARS coronavirus. Nature 426 (6965), 450–454.

Marra, M.A., Jones, S.J., Astell, C.R., Holt, R.A., Brooks-Wilson, A., Butterfield, Y.S., Khattra, J., Asano, J.K., Barber, S.A., Chan, S.Y., Cloutier, A., Coughlin, S.M., Freeman, D., Girn, N., Griffith, O.L., Leach, S.R., Mayo, M., McDonald, H., Montgomery, S.B., Pandoh, P.K., Petrescu, A.S., Robertson, A.G., Schein, J.E., Siddiqui, A., Smailus, D.E., Stott, J.M., Yang, G.S., Plummer, F., Andonov, A., Artsob, H., Bastien, N., Bernard, K., Booth, T.F., Bowness, D., Czub, M., Drebot, M., Fernando, L., Flick, R., Garbutt, M., Gray, M., Grolla, A., Jones, S., Feldmann, H., Meyers, A., Kabani, A., Li, Y., Normand, S., Stroher, U., Tipples, G.A., Tyler, S., Vogrig, R., Ward, D., Watson, B., Brunham, R.C., Krajden, M., Petric, M., Skowronski, D.M., Upton, C., Roper, R.L., 2003. The Genome sequence of the SARS-associated coronavirus. Science 300 (5624), 1399–1404.

Meeusen, E.N., Scheerlinck, J.P., Wattegedera, S., Entrican, G., 2004. Advances in mucosal vaccination. Anim. Health Res. Rev. 5 (2), 209–217.

Mizutani, T., Fukushi, S., Saijo, M., Kurane, I., Morikawa, S., 2004. Phosphorylation of p38 MAPK and its downstream targets in SARS coronavirus-infected cells. Biochem. Biophys. Res. Commun. 319 (4), 1228–1234.

Nal, B., Chan, C., Kien, F., Siu, L., Tse, J., Chu, K., Kam, J., Staropoli, I., Crescenzo-Chaigne, B., Escriou, N., van der Werf, S., Yuen, K.Y., Altmeyer, R., 2005. Differential maturation and subcellular localization of severe acute respiratory syndrome coronavirus surface proteins S, M and E. J. Gen. Virol. 86 (Pt. 5), 1423–1434.

Nam, J.H., Wyatt, L.S., Chae, S.L., Cho, H.W., Park, Y.K., Moss, B., 1999. Protection against lethal Japanese encephalitis virus infection of mice by immunization with the highly attenuated MVA strain of vaccinia virus expressing JEV prM and E genes. Vaccine 17 (3), 261–268.

Ohnishi, K., Sakaguchi, M., Kaji, T., Akagawa, K., Taniyama, T., Kasai, M., Tsunetsugu-Yokota, Y., Oshima, M., Yamamoto, K., Takasuka, N., Hashimoto, S., Ato, M., Fujii, H., Takahashi, Y., Morikawa, S., Ishii, K., Sata, T., Takagi, H., Itamura, S., Odagiri, T., Miyamura, T., Kurane, I., Tashiro, M., Kurata, T., Yoshikura, H., Takemori, T., 2005. Immunological

detection of severe acute respiratory syndrome coronavirus by monoclonal antibodies. Jpn. J. Infect. Dis. 58 (2), 88–94.

Peiris, J.S., Lai, S.T., Poon, L.L., Guan, Y., Yam, L.Y., Lim, W., Nicholls, J., Yee, W.K., Yan, W.W., Cheung, M.T., Cheng, V.C., Chan, K.H., Tsang, D.N., Yung, R.W., Ng, T.K., Yuen, K.Y., 2003. Coronavirus as a possible cause of severe acute respiratory syndrome. Lancet 361 (9366), 1319–1325.

Rota, P.A., Oberste, M.S., Monroe, S.S., Nix, W.A., Campagnoli, R., Icenogle, J.P., Penaranda, S., Bankamp, B., Maher, K., Chen, M.H., Tong, S., Tamin, A., Lowe, L., Frace, M., DeRisi, J.L., Chen, Q., Wang, D., Erdman, D.D., Peret, T.C., Burns, C., Ksiazek, T.G., Rollin, P.E., Sanchez, A., Liffick, S., Holloway, B., Limor, J., McCaustland, K., Olsen-Rasmussen, M., Fouchier, R., Gunther, S., Osterhaus, A.D., Drosten, C., Pallansch, M.A., Anderson, L.J., Bellini, W.J., 2003. Characterization of a novel coronavirus associated with severe acute respiratory syndrome. Science 300 (5624), 1394–1399.

Ruan, Y.J., Wei, C.L., Ee, A.L., Vega, V.B., Thoreau, H., Su, S.T., Chia, J.M., Ng, P., Chiu, K.P., Lim, L., Zhang, T., Peng, C.K., Lin, E.O., Lee, N.M., Yee, S.L., Ng, L.F., Chee, R.E., Stanton, L.W., Long, P.M., Liu, E.T., 2003. Comparative full-length genome sequence analysis of 14 SARS coronavirus isolates and common mutations associated with putative origins of infection. Lancet 361 (9371), 1779–1785.

Seo, S.H., Wang, L., Smith, R., Collisson, E.W., 1997. The carboxyl-terminal 120-residue polypeptide of infectious bronchitis virus nucleocapsid induces cytotoxic T lymphocytes and protects chickens from acute infection. J. Virol. 71 (10), 7889–7894.

Someya, K., Xin, K.Q., Matsuo, K., Okuda, K., Yamamoto, N., Honda, M., 2004. A consecutive priming-boosting vaccination of mice with simian immunodeficiency virus (SIV) gag/pol DNA and recombinant vaccinia virus strain DIs elicits effective anti-SIV immunity. J. Virol. 78 (18), 9842–9853.

Stittelaar, K.J., Wyatt, L.S., de Swart, R.L., Vos, H.W., Groen, J., van Amerongen, G., van Binnendijk, R.S., Rozenblatt, S., Moss, B., Osterhaus, A.D., 2000. Protective immunity in macaques vaccinated with a modified vaccinia virus Ankara-based measles virus vaccine in the presence of passively acquired antibodies. J. Virol. 74, 4236–4243.

Storch, G.A., 2001. Diagnostic virology. In: David, P.M.H., Knipe, M. (Eds.), Fields Virology, 4th ed. Lippincott Williams & Wilkins, Philadelphia, PA, pp. 493–531.

Subbarao, K., McAuliffe, J., Vogel, L., Fahle, G., Fischer, S., Tatti, K., Packard, M., Shieh, W.J., Zaki, S., Murphy, B., 2004. Prior infection and passive transfer of neutralizing antibody prevent replication of severe acute respiratory syndrome coronavirus in the respiratory tract of mice. J. Virol. 78 (7), 3572–3577.

Sutter, G., Moss, B., 1992. Nonreplicating vaccinia vector efficiently expresses recombinant genes. Proc. Natl. Acad. Sci. U. S. A. 89, 10847–10851.

Sutter, G., Wyatt, L.S., Foley, P.L., Bennink, J.R., Moss, B., 1994. A recombinant vector derived from the host range-restricted and highly attenuated MVA strain of vaccinia virus stimulates protective immunity in mice to influenza virus. Vaccine 12, 1032–1040.

Tagaya, I., Kitamura, T., Sano, Y., 1961. A new mutant of dermovaccinia virus. Nature 192, 381–382.

Takasuka, N., Fujii, H., Takahashi, Y., Kasai, M., Morikawa, S., Itamura, S., Ishii, K., Sakaguchi, M., Ohnishi, K., Ohshima, M., Hashimoto, S., Odagiri, T., Tashiro, M., Yoshikura, H., Takemori, T., Tsunetsugu-Yokota, Y., 2004. A subcutaneously injected UV-inactivated SARS coronavirus vaccine elicits systemic humoral immunity in mice. Int. Immunol. 16 (10), 1423–1430.

Weingartl, H., Czub, M., Czub, S., Neufeld, J., Marszal, P., Gren, J., Smith, G., Jones, S., Proulx, R., Deschambault, Y., Grudeski, E., Andonov, A., He, R., Li, Y., Copps, J., Grolla, A., Dick, D., Berry, J., Ganske, S., Manning, L., Cao, J., 2004. Immunization with modified vaccinia virus Ankara-based recombinant vaccine against severe acute respiratory syndrome is associated with enhanced hepatitis in ferrets. J. Virol. 78 (22), 12672–12676.

Weisz, O.A., Swift, A.M., Machamer, C.E., 1993. Oligomerization of a membrane protein correlates with its retention in the Golgi complex. J. Cell Biol. 122 (6), 1185–1196.

Wyatt, L.S., Shors, S.T., Murphy, B.R., Moss, B., 1996. Development of a replication-deficient recombinant vaccinia virus vaccine effective against parainfluenza virus 3 infection in an animal model. Vaccine 14 (15), 1451–1458.

Xiao, X., Chakraborti, S., Dimitrov, A.S., Gramatikoff, K., Dimitrov, D.S., 2003. The SARS-CoV S glycoprotein: expression and functional characterization. Biochem. Biophys. Res. Commun. 312 (4), 1159–11564.

Yang, Z.Y., Kong, W.P., Huang, Y., Roberts, A., Murphy, B.R., Subbarao, K., Nabel, G.J., 2004. A DNA vaccine induces SARS coronavirus neutralization and protective immunity in mice. Nature 428 (6982), 561–564.

Yang, Z.Y., Werner, H.C., Kong, W.P., Leung, K., Traggiai, E., Lanzavecchia, A., Nabel, G.J., 2005. Evasion of antibody neutralization in emerging severe acute respiratory syndrome coronaviruses. Proc. Natl. Acad. Sci. U. S. A. 102 (3), 797–801.

Yoshizawa, I., Soda, Y., Mizuochi, T., Yasuda, S., Rizvi, T.A., Takemori, T., Tsunetsugu-Yokota, Y., 2001. Enhancement of mucosal immune response against HIV-1 Gag by DNA immunization. Vaccine 19 (20–22), 2995–3003.

You, J., Dove, B.K., Enjuanes, L., DeDiego, M.L., Alvarez, E., Howell, G., Heinen, P., Zambon, M., Hiscox, J.A., 2005. Subcellular localization of the severe acute respiratory syndrome coronavirus nucleocapsid protein. J. Gen. Virol. 86 (Pt. 12), 3303–3310.

Zakhartchouk, A.N., Viswanathan, S., Mahony, J.B., Gauldie, J., Babiuk, L.A., 2005. Severe acute respiratory syndrome coronavirus nucleocapsid protein expressed by an adenovirus vector is phosphorylated and immunogenic in mice. J. Gen. Virol. 86 (Pt. 1), 211–215.

Zhao, P., Cao, J., Zhao, L.J., Qin, Z.L., Ke, J.S., Pan, W., Ren, H., Yu, J.G., Qi, Z.T., 2005. Immune responses against SARS-coronavirus nucleocapsid protein induced by DNA vaccine. Virology 331 (1), 128–135.

Zhi, Y., Kobinger, G.P., Jordan, H., Suchma, K., Weiss, S.R., Shen, H., Schumer, G., Gao, G., Boyer, J.L., Crystal, R.G., Wilson, J.M., 2005. Identification of murine CD8 T cell epitopes in codon-optimized SARS-associated coronavirus spike protein. Virology 335 (1), 34–45.

Zhu, M.S., Pan, Y., Chen, H.Q., Shen, Y., Wang, X.C., Sun, Y.J., Tao, K.H., 2004. Induction of SARS-nucleoprotein-specific immune response by use of DNA vaccine. Immunol. Lett. 92 (3), 237–243.

Jpn. J. Infect. Dis., 58, 88-94, 2005

Original Article

Immunological Detection of Severe Acute Respiratory Syndrome Coronavirus by Monoclonal Antibodies

Kazuo Ohnishi, Masahiro Sakaguchi, Tomohiro Kaji, Kiyoko Akagawa, Tadayoshi Taniyama, Masataka Kasai, Yasuko Tsunetsugu-Yokota, Masamichi Oshima, Kiichi Yamamoto, Naomi Takasuka, Shu-ichi Hashimoto, Manabu Ato, Hideki Fujii, Yoshimasa Takahashi, Shigeru Morikawa[1], Koji Ishii[2], Tetsutaro Sata[4], Hirotaka Takagi[5], Shigeyuki Itamura[3], Takato Odagiri[3], Tatsuo Miyamura[2], Ichiro Kurane[1], Masato Tashiro[3], Takeshi Kurata[6], Hiroshi Yoshikura[6] and Toshitada Takemori*

Department of Immunology, [1]Department of Virology I, [2]Department of Virology II, [3]Department of Virology III, [4]Department of Pathology and [5]Division of Biosafety Control and Research, [6]National Institute of Infectious Diseases, Tokyo 162-8640, Japan

(Received October 20, 2004. Accepted February 14, 2005)

SUMMARY: In order to establish immunological detection methods for severe acute respiratory syndrome coronavirus (SARS-CoV), we established monoclonal antibodies directed against structural components of the virus. B cell hybridomas were generated from mice that were hyper-immunized with inactivated SARS-CoV virion. By screening 2,880 generated hybridomas, we established three hybridoma clones that secreted antibodies specific for nucleocapsid protein (N) and 27 clones that secreted antibodies specific for spike protein (S). Among these, four S-protein specific antibodies had in vitro neutralization activity against SARS-CoV infection. These monoclonal antibodies enabled the immunological detection of SARS-CoV by immunofluorescence staining, Western blot or immunohistology. Furthermore, a combination of monoclonal antibodies with different specificities allowed the establishment of a highly sensitive antigen-capture sandwich ELISA system. These monoclonal antibodies would be a useful tool for rapid and specific diagnosis of SARS and also for possible antibody-based treatment of the disease.

INTRODUCTION

The outbreak of severe acute respiratory syndrome (SARS) in 2003, caused by SARS coronavirus (SARS-CoV)(1,2), ultimately led to 8,000 people becoming infected, 916 of whom died (3; http://who.int/csr/sars/country/en/country2003_08_15.pdf). Even though the WHO announced an end to the epidemic (4; http://www.who.int/entity/csr/sars/resources/en/SARSReferenceLab1.pdf), the threat of re-emergence persists due to the absence of a vaccine, and inability of health services to rapidly detect and specifically diagnose the disease. One of the critical issues in the management of clinical patients and control of the pandemic is a system of early diagnosis that distinguishes SARS from other types of pulmonary infections. As an epidemiological history of contact with SARS patients is not always provable and there are no clinical signs unique to SARS patients (5), confirmatory diagnosis relies primarily on laboratory tests.

To date, viral shedding of SARS-CoV has been extensively studied to improve diagnosis and infectious control (6-8). Maximum virus shedding takes place between day 12 and day 14 of disease onset. For most acute respiratory viral infections, viral shedding occurs within the first few days from the nasopharyngeal tissue and soon after at the upper respiratory tract, but seldom lasts for more than 10 days (6-8). The peak of shedding in stools occurs a few days after respiratory shedding and remains high even after 3 weeks (7, 8). SARS-CoV was detected in patients' plasma samples within several days of the onset of fever, sometimes at levels equivalent to those recorded for nasopharyngeal aspirates (6, 9).

Previously, during the outbreak in Hong Kong (8), laboratory diagnosis for SARS virus infection was based on a combination of serologic tests, reverse transcription-polymerase chain reaction (RT-PCR), and virus isolation. IgG seroconversion among those infected was 93% by day 28 (5), suggesting that while antibody seroconversion provides reliable proof of infection (5,10); it is, however, not suitable for early diagnosis (11). Among patients in whom the serological evidence could be retrospectively examined, RT-PCR provided about 60% of the diagnostic yield using tracheal aspirates and stools for the first 2 weeks after the onset of illness (8). Although the availability of data that compares the diagnostic yield of various specimen types is still limited, it has been suggested that a combination of stool samples and pooled throat and nasal swab specimens provides reagents for safe and high-yield SARS-CoV detection (8). Furthermore, in addition to RT-PCR on respiratory and fecal samples, serology is needed to confirm the diagnosis of SARS-CoV infection in most cases.

Based on clinical experience, several options have been considered in the quest to develop the capacity to accurately diagnose SARS-CoV infection, including molecular biology techniques and serological tests such as antigen-captured ELISA assay and immunofluorescence assay to detect virus-infected cells in respiratory swabs (5-12). The preparation of monoclonal antibodies (mAbs) is considered to be valuable especially for serological testing.

*Corresponding author: Mailing address: Department of Immunology, National Institute of Infectious Diseases, Toyama 1-23-1, Shinjuku-ku, Tokyo 162-8640, Japan. Tel: +81-3-5285-1111, Fax: +81-5285-1150. E-mail: ttoshi@nih.go.jp

In this paper we report the successful establishment and the characterization of mAbs against SARS-CoV structural components. These mAbs enabled the general immunological detection of SARS-CoV, by the methods such as immunofluorescent staining, Western blotting, and immunohistology, in addition to the construction of highly sensitive antigen-capture sandwich ELISA.

MATERIALS AND METHODS

Virus and cell culture: SARS-CoV (HKU-39849) was kindly supplied by Dr. J. S. M. Peiris, Department of Microbiology, the University of Hong Kong. The live virus was manipulated under the physical containment level P3. For the purification of the virion, the day-2 culture supernatant of Vero E6, which had been infected with SARS-CoV at moi = 1.0, was centrifuged at 8,000×g for 30 min to remove cell debris. The virion in the supernatant was precipitated with 8% polyethylene glycol/ 0.5 M NaCl, and further purified by 20%/60%-discontinuous sucrose density gradient centrifugation. This fraction was inactivated by UV-irradiation (260 nm, 4.75 J/cm^2), and used as UV-inactivated SARS-CoV fraction. We and others confirmed that this condition completely inactivates SARS-CoV (13,14).

Production of mAbs: BALB/c mice (9-week old females, Japan SLC) were immunized subcutaneously with 20 μg of UV-inactivated SARS-CoV using Freund's Complete Adjuvant (FCA, Sigma, St. Louis, Mo., USA). After 2 weeks, the mice were boosted with a subcutaneous injection of 5 μg of UV-inactivated SARS-CoV using Freund's Incomplete Adjuvant (FIA, Sigma). On day-3 after the boost, sera from the mice were tested by ELISA for the antibody titer against SARS-CoV. The two mice showing highest antibody titer were further boosted intravenously with 5 μg of the inactivated virus 14 days after the previous boost. This immunization schedule was called protocol-1. In protocol-2 the booster injection was repeated two more times before the final boost. Three days after the final boost, spleens from two mice were excised and the splenocytes were fused with Sp2/O-Ag14 myeloma by the polyethylene glycol method of Kozbor and Roder (15). The fused cells from the two spleens were cultured and HAT-selected on twenty 96-well plates. The first screening was conducted by ELISA using SARS-CoV infected Vero E6 cell lysate as the antigen. In this first screening, the ELISA with uninfected Vero E6 cell lysate was used as the negative control. After the virus was inactivated by UV-irradiation, cell lysates were prepared by NP-40 lysis buffer (1% NP-40/ 150 mM NaCl/ 50 mM Tris, pH 7.5) followed by centrifugation at 15,000 rpm for 20 min to remove the cell debris. The supernatant was diluted 100-fold using ELISA-coating buffer (50 mM sodium bicarbonate, pH 9.6) and the ELISA plates (Dynatech, Chantily, Va., USA) were coated at 4°C overnight. After blocking with 1% ovalbumin in PBS-Tween (10 mM phosphate buffer, 140 mM NaCl, 0.05% Tween 20, pH 7.5) for 1 h, the culture supernatants from HAT-selected hybridomas were added and incubated for 1 h. After washing with PBS-Tween, the bound antibodies were detected with alkaline phosphatase-conjugated anti-mouse IgG (1:2000, Zymed, South San Francisco, Calif., USA) using *p*-nitrophenyl phosphate (PNPP) as a substrate. The second screening was conducted by ELISA using the cell lysates of chick embryonic fibroblast (CEF) cell lines that were transfected by vaccinia virus vector containing the gene either of SARS-CoV spike (S) or nucleocapsid (N) proteins.

Recombinant virus proteins: Genomic RNA was extracted from SARS-CoV strain HKU39849 and reverse transcribed to cDNA. The corresponding open reading frames (ORF) to E, M, N and S were amplified by PCR and cloned into the transfer vector, pDIsgptmH5, which also harbored *Escherichia coli* xantine-guanine phosphoribosyltransferase under the control of vaccinia virus p7.5 promoter in the cloning site of pUc/DIs (16). The recombinant clones of attenuated vaccinia virus, DIs, which harbored each ORF were obtained by homologous recombination induced in DIs-infected-, pDIsgptmH5-transfected CEF cells. The detailed protocol will be published elsewhere.

Neutralization assay: The known tissue culture infectious dose (TCID) of SARS-CoV was incubated for 1 h in the presence or absence of the purified mAbs serially diluted 10-fold, and then added to Vero E6 cell culture grown to confluence in a 96-well microtiter plate. As a control, mAbs against N protein was added to the culture. After 48 hr, cells were fixed with 10% formaldehyde and stained with crystal violet to visualize the cytopathic effect induced by the virus (17). Neutralization antibody titers were expressed as the minimum concentration of purified immunoglobulin that inhibits cytopathic effect.

Western blot: UV-inactivated purified SARS-CoV virion (0.5 μg/lane)(13) was loaded on SDS-PAGE under reduced conditions. Proteins were transferred to the PVDF membrane (Genetics, Tokyo, Japan). After blocking with BlockAce (Snow Brand Milk Products Co., Ltd., Tokyo, Japan) reagent, the membranes were reacted with the mAbs or the diluted sera (1:1000) that had been obtained from mice inoculated with UV-irradiated SARS-CoV. After washing, the membrane was reacted with peroxidase-conjugated F(ab')$_2$ fragment anti-mouse IgG (H+L) (1:20,000 Jackson Immuno Research, West Grove, Pa., USA), and the bands were visualized using chemiluminescent reagents (Amasham Biosciences, Piscataway, N.J., USA) on the X-ray film (Kodak, Rochester, N.Y., USA).

Purification and biotinylation of mAbs: Hybridomas were grown in Hybridoma-SFM medium (Invitrogen, Carlsbad, Calif., USA) supplemented with recombinant IL-6 (18) and penicillin (100 U/mL)/streptomycin (100 μg/mL). The culture supernatants were harvested, added with 1/100 volume of 1 M Tris-HCl (pH 7.4) and 1/500 volume of 10% NaN_3, and directly loaded on the Protein G-Sepharose 6B column (Amersham Biosciences). The column was washed with PBS and eluted with Glycine/HCl (pH 2.8). After measuring the OD_{280} of the fractions, protein containing fractions were pooled and added with an equal volume of saturated $(NH_4)_2SO_4$. Precipitated proteins were dissolved in PBS, dialysed against PBS and stored at −20°C. The purified antibodies were biotinylated using sulfo-NHS-LC-biotin (Pierce, Rockford, Ill., USA) according to the manufacturer's protocol.

Antigen-capture ELISA: The purified mAb for the antigen-capture was immobilized on the microplate (Immulon 2, Dynatech) by incubating 4 μg/mL antibody in 50 mM sodium bicarbonate buffer (pH 8.6) at 4°C overnight. The microplate was blocked with 1% BSA, washed with PBS-Tween, and reacted with serial dilution of UV-inactivated purified SARS-CoV for 1 h at room temperature. After washing with PBS-Tween, wells were reacted with biotinylated probing mAb (0.1 μg/mL) for 1 h at room temperature. After washing, wells were reacted with β-D-galactosidase-labeled streptavidine (Zymed) for 1 h at room temperature. After washing,

fluorescent substrate 4-methylumberyferyl-β-D-galactoside (Sigma-Aldrich, St. Louis, Mo., USA) was added and the substrate was incubated for 2 h at 37°C. The reaction was stopped by adding 0.1M Glycine-NaOH (pH 10.2) and the fluorescence (FU) of the reaction product, 4-methylumbriferron, was measured using FluoroScan (Flow Laboratories Inc., Inglewood, Calif., USA).

Histology: Formaldehyde-fixed human lung tissue that was RT-PCR positive for SARS-CoV (19) and lung from a SARS-CoV infected macaque were embedded in paraffin and sectioned using the standard method. After de-paraffinization by standard method, the sections were soaked with 0.1 M citrate-buffer (pH 6.0) and autoclaved for 10 min at 121°C to inactivate viruses. Endogenous peroxidase was inactivated by 0.3% hydrogen peroxide for 30 min at room temperature. After blocking with 5% normal goat serum for 10 min, sections were incubated with the mAb at 4°C overnight. The bound antibody was detected by biotinylated anti-mouse IgG followed by peroxidase-labeled streptavidin (LSAB2 kit, DakoCytomation, Kyoto, Japan) and visualized with 0.2 mg/mL 3,3′-diaminobenzidine in 0.015% hydrogen peroxide/0.05M Tris-HCl (pH 7.6). The sections were counterstained with hematoxylin.

RESULTS

In order to establish the hybridomas that secrete specific mAbs to SARS-CoV, we immunized BALB/c mice with purified SARS-CoV whole virion fraction. The virus was inactivated by UV-irradiation to avoid a change in antigenicity presumably caused by aldehyde-fixation or detergent-solubilization. The immunization protocols used were those of the standard method in which the boost administrations were repeated twice (protocol-1) or four times (protocol-2) with 2-week intervals using FCA/FIA as an adjuvant (see Materials and Methods). Three days after the final boost, a single cell suspension was prepared from two spleens of immunized mice and fused with SP-2/O myeloma by a polyethylene-glycol method, the fused cells were then HAT-selected (15).

In the experiment with immunization protocol-1, we found that the culture supernatants from 28 of the 1,920 wells were strong-positive in ELISA testing in which the cell-lysate of SARS-CoV infected Vero E6 cells was used as a coated antigen (Table 1). As a negative control, we used uninfected Vero E6 cell-lysate as the antigen. Wells that showed a positive reaction were omitted from the count. Among the 28 wells, 19 reacted to vaccinia vector-based recombinant-S-protein and three reacted to recombinant-N-protein. These hybridomas were successfully cloned by a repeated limiting dilution method. The remaining six wells did not give rise to a significant positive signal to recombinant-S, -N or -M proteins. One anti-S mAb cross-reacted to porcine transmissible gastroenteritis virus (TGEV) and this clone was also omitted from further studies. None of these mAbs cross-reacted to mouse hepatitis virus (MHV).

The avidities of these cloned mAbs were tested by avidity-ELISA in the presence of urea. Although in the presence of 6 M urea some anti-S mAbs retained 18-35% of the original reactivity, less than 10% of the original reactivity remained in the presence of 8 M urea (Table 2). Three anti-N mAbs showed a very low avidity index in this assay system.

In a previous report that studied human IgG avidity maturation after rubella vaccination, high-avidity antibodies were defined as those that retain more than 50% of reactivity in the presence of 8 M urea (20). Although it would not be possible to directly apply this definition of polyclonal antibodies to our mAb case, the avidities of mAbs we obtained did not seem particularly high. This prompted us to attempt to obtain better mAbs with higher avidity by repeating booster immunization in anticipation of affinity maturation. After an additional two boosts, hybridomas were established by the same procedure as the first experiment. We screened 960 wells and obtained 14 wells positive for ELISA with SARS-CoV infected Vero E6 cell lysate (Table 1). Among the 14 wells, seven reacted with recombinant-S protein and none of them reacted with recombinant-N or -M proteins. These anti-S antibodies showed significantly higher avidity in the avidity ELISA (two representative clones are shown in Table 2). From the results of this avidity test, we selected five anti-S mAbs that showed the highest avidity index. None of these mAbs cross-reacted to human coronavirus, 229E (data not shown). These five anti-S and three anti-N mAbs were purified, and characterized further.

Table 1. Summary of the first hybridoma screening by ELISA

Immobilized antigen	Experiment-1[1)]	Experiment-2[2)]	Total
(Total wells assayed)	1,920	960	2,880
SARS-CoV infected Vero cell-lysate	28	14	42
Recombinant - S	19	7	26
- N	3	0	3

[1)]: Immunization protocol-1
[2)]: Immunization protocol-2

Table 2. Avidity ELISA

Clone	Epitope	Avidity Index (%)		
		4M urea	6M urea	8M urea
Experiment-1				
SKOT-7	N	1.6	1.2	1.5
SKOT-8	N	2.3	3.2	3.7
SKOT-9	N			
SKOT-3	S	45.5	18.7	1.2
SKOT-10	S	73.4	29.9	2.6
SKOT-20	S	63.8	35.4	8.8
Experiment-2				
SOAT-5	S	51.3	48.0	43.3
SOAT-13	S	77.0	62.0	48.0

All selected mAbs worked successfully in the immunofluorescent staining assay (Fig. 1). Anti-S mAbs such as SKOT-3, -10, -20, SOAT-5 and -13 stained the Golgi body and surface membrane of virus-infected cells but not of uninfected-cells. In contrast, the staining patterns of anti-N mAbs such as SKOT-7, -8 and -9 were mainly confined to the Golgi body.

All anti-N mAbs worked in immunohistochemistry of formalin-fixed, paraffin-embedded sections of both human lung from SARS patients and SARS-CoV infected macaque lung (Fig. 2). The specificity of these stainings was confirmed by the negative results for normal lungs and several specimens from pneumonia patients including cases complicated by measles, influenza type A, herpes-simplex and herpes zoster.

The mAbs that worked for immunohistochemistry, i.e.,

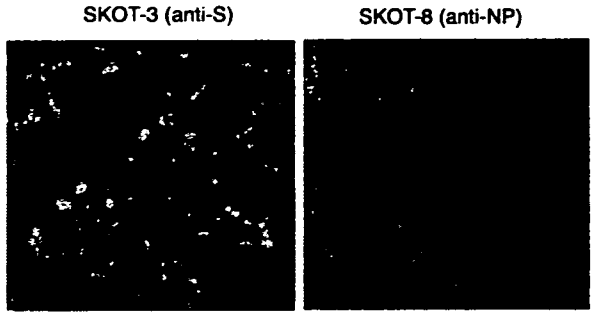

Fig. 1. Fluorescent immunostaining of SARS-CoV infected Vero E6 cells with monoclonal antibodies (mAbs). Parformaldehyde-fixed, SARS-CoV infected Vero E6 cells were permeabilized with TBS-tween and incubated with mAbs from hybridoma clones and the antibodies were detected with FITC-conjugated anti-mouse IgG. Shown are representative staining patterns with anti-S mAb, SKOT-3 (A), and anti-N mAb, SKOT-8 (B).

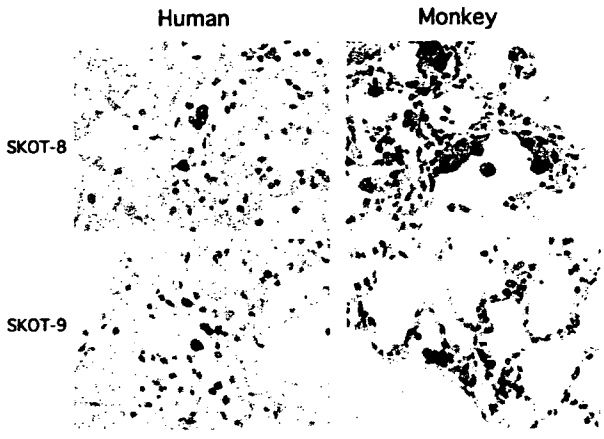

Fig. 2. Immuno-histochemistry of SARS-CoV infected human lung and macaque lung tissues with mAbs. Paraformaldehyde-fixed, paraffin-embedded sections were incubated with mAbs, and then with biotinylated anti-mouse IgG/peroxidase-labeled streptavidin complex before being visualized using DAB as a peroxidase substrate. Counter-staining with hematoxilin. Shown are human patient lung tissue (left panels) and SARS-infected macaque lung tissues (right panels), stained with anti-N mAbs (SKOT-8, SKOT-9).

SKOT-7, -8 and -9 also worked for Western-blot detection of the viral proteins (Fig. 3). Anti-N mAbs detected a band of 50 kDa that corresponds to the calculated molecular weight of SARS-CoV N-protein. In some experiments with longer exposure, a band with an apparent molecular weight of 120 kDa was also detected. None of the anti-S mAbs worked in the Western blot, suggesting that the major antigenic determinants of the S-protein are 'conformational' epitopes.

We tested the in vitro neutralizing activities of anti-S mAbs. As shown in Fig. 4, SKOT-20 neutralized in vitro SARS-CoV infection to Vero E6 cells at an antibody concentration of 1 μg/mL. Another anti-S mAb, SKOT-19, which had a low avidity value, also showed similar neutralizing activity. SKOT-10 and -3 also had neutralization activity but required higher antibody concentrations.

Lastly, we tried to construct an antigen-capture detection system for SARS-CoV by sandwich ELISA. In preliminary experiments, we tested all the combinations of two mAbs from the selected eight mAbs to obtain the highest detection sensitivity for purified SARS-CoV virion, and found that the

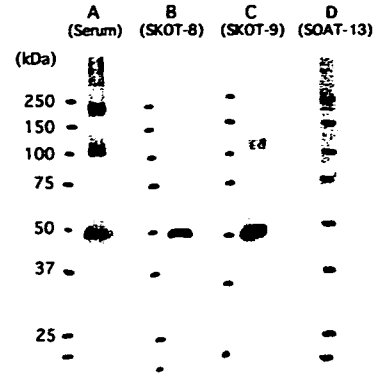

Fig. 3. Detection of virus proteins with Western blot. Purified SARS-CoV proteins (0.5 μg/lane) were electrophoresed with SDS-PAGE under reducing conditions. After blotting on the PVDF membrane, proteins were detected by incubation with mAbs, followed by incubation with peroxidase labeled-F(ab')$_2$ fragment of Donkey anti-mouse IgG. They were then visualized by chemiluminescent reaction. A: mouse serum from SARS-CoV immunized mouse; B: anti-N mAb, SKOT-8; C: anti-N mAb, SKOT-9; D: anti-S mAb, SOAT-13. The positions of molecular weight markers are shown on the left.

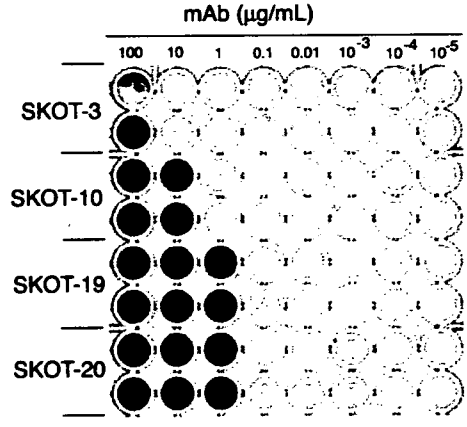

Fig. 4. In vitro neutralization assay of SARS-CoV infection with mAbs. Purified SARS-CoV fraction was diluted to 1 × 10^2 PFU/mL and incubated with serially-titrated purified mAbs for 1 h at 37°C. After the reaction, samples were poured into wells of a 96-well plate on which Vero E6 cells were grown to 90% confluent. After 48 h, cytotoxicities were visualized by staining the cells with crystalviolet. The results of purified anti-S antibodies (SKOT-3, -10, -19 and -20) with concentrations ranging from 100 μg/mL to 10^{-5} μg/mL are shown.

immobilization of SKOT-8 on the ELISA plate followed by the detection with biotinylated SKOT-9 gave the best result (data not shown; see Materials and Methods). In this sandwich ELISA, SARS-CoV protein was successfully detected in a concentration as low as 40 pg/mL (Fig. 5). Since the mAbs were originally raised against SARS-CoV strain HKU39849, we tested the validity of this system for other strains of SARS-CoV. As shown in Fig. 6, it was confirmed that the strains HK14T1WL, CDC00592 and Frankfurt1 were as detectable as HKU39849 using this system.

DISCUSSION

We established mAbs against SARS-CoV, which enable

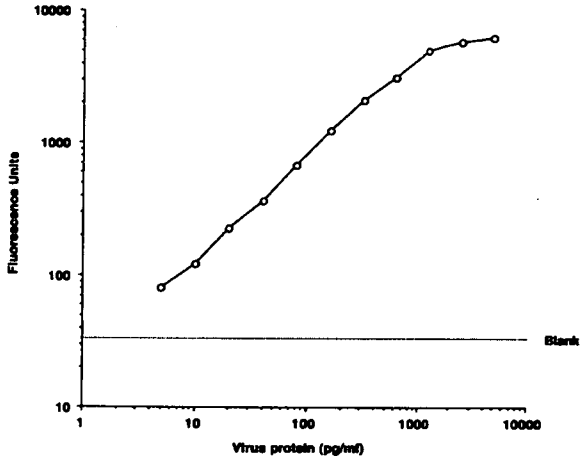

Fig. 5. Antigen-capture ELISA of SARS-CoV with mAbs. Anti-N mAb, SKOT-8, was immobilized on the surface of a 96 well plate. Serially-titrated purified SARS-CoV fractions were reacted for 1 h at room temperature and the bound virus proteins were detected by biotinylated SKOT-9 (anti-N) antibody followed by peroxydase-labeled streptavidin. They were then quantitated by chemiluminescent reaction using 4-methylumberiferril as a substrate. Abscissa: concentration of purified SARS-CoV proteins; ordinate: fluorescent unit.

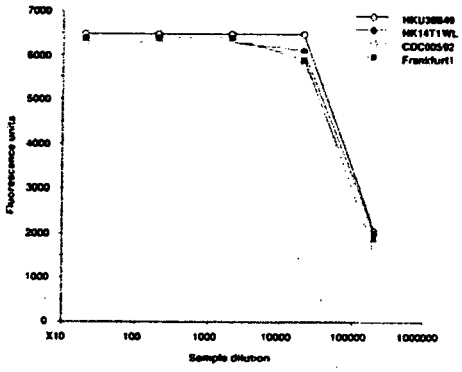

Fig. 6. Comparison of SARS-CoV strains for reactivity to the antigen capture sandwich ELISA. SARS-CoV strains, HKU39849, HK14T1WL, CDC00592 and Frankfurt1 were tested for the reactivity to the antigen-capture ELISA system as described in Fig. 5. Abscissa: sample dilution; ordinate: fluorescent units.

the detection of virus S- and N-proteins by means of immunofluorescence assay, immunohistochemistry, Western blot and antigen-capture ELISA. A summary of selected mAbs is shown in Table 3.

Among the originally selected 42 mAbs that were positive in ELISA for SARS-CoV infected Vero E6 cell lysate, 26 reacted to recombinant-S-protein and only three reacted to N-protein. We could not find hybridoma secreting mAb to M-protein or other protein components of SARS-CoV. These results suggest that S protein is the dominant target in the antibody response. We observed that none of the anti-S mAbs established worked in Western blot, suggesting that these mAbs may recognize 'conformational' epitopes. In contrast, all three anti-N mAbs worked in Western blot and immunohistochemistry, suggesting that these mAbs recognize 'linear' epitopes.

We examined whether our mAbs were applicable for immunofluorescence detection of virus-infected cells. In immunofluorescent staining of Vero E6 cells infected with SARS-CoV, anti-N mAbs stained the Golgi body and anti-S mAbs stained the Golgi body and surface membrane. This difference in localization of N- and S-proteins may reflect the common assembly process of coronaviruses (21). Further analysis is needed to clarify sensitivity and specificity in infected cells for clinical use.

During the course of outbreak of SARS-CoV in Hong Kong, it was reported that more than half the patients were not positively diagnosed by RT-PCR (8). Therefore, the diagnosis was finally confirmed by serum specimens in a convalescent-phase at a late stage of illness (8). To overcome this problem, virus shedding patterns have been extensively analyzed, with results showing that respiratory shedding of the virus increases over the first week and viral shedding in stools begins a few days after respiratory shedding (7,8). From this analysis, it is considered that a combination of stool sampling and pooled throat and nasal swab specimens could be good specimens for safe and highly sensitive SARS-CoV detection.

In general, a single diagnostic test is not conclusively reliable, because of the serious potential for false positives and negatives. Considering the limited sensitivity of RT-PCR, serological screening systems other than antibody detection are currently being examined (22,23). ELISA-based antigen captured assays are known to offer high specificity and reproducibility. Antigen-captured assays have been used in the diagnosis and monitoring of disease in cases of infection with dengue virus (24), human immunodeficient virus p24 (25) and Ebola hemorragic fever (26) and examined in hepatitis B virus and hepatitis C virus (22,23). In this context, extensive analysis in Ebola hemorragic fever suggests that the RT-PCR assay is extremely useful, but should always be utilized in combination with antigen-captured ELISA, which makes the diagnosis more reliable (26).

Table 3. Summary of selected hybridoma clones

Clone	Epitope	Class	IFA	Neutralization[1]	Western-blot	Histology	Avidity (%)[2]
SKOT-7	N	IgG	Golgi	-	50kDa	-	1.2
SKOT-8	N	IgG	Golgi	-	50kDa	Usable	3.2
SKOT-9	N	IgG	Golgi	-	120, 50kDa	Usable	3.8
SKOT-3	S	IgG	Golgi / cell membrane	100	-	-	18.7
SKOT-10	S	IgG	Golgi / cell membrane	10	-	-	29.9
SKOT-19	S	IgG	Golgi / cell membrane	1	ND	ND	ND
SKOT-20	S	IgG	Golgi / cell membrane	1	-	-	35.4
SOAT-5	S	IgG	Golgi / cell membrane	ND	-	-	48.0
SOAT-13	S	IgG	Golgi / cell membrane	ND	-	-	62.0

[1]: Numbers represent minimum concentration (μg/mL) that exerts neutralization. -, no neutralization activity; ND, not determined.
[2]: Avidity index at 6M urea (see Materials and Methods).

In the case of SARS-CoV, the assay has been recently evaluated by using mAbs and polyclonal antibodies directed against recombinant SARS-CoV nucleocapsid protein (22,23). A soluble N-protein was observed to be released from infected cells in culture, which led to the opportunity to evaluate the level in serum specimens from infected patients. N-antigen ELISA employing mAbs reproducibly detected 50% of patients on days 3 and 5 after the onset of illness, with a limitation of the detection of the recombinant protein at 50 pg/ml (22). N-antigen ELISA with use of polyclonal antibodies detected 60-50% of nasopharyngeal aspirate and fecal specimens from patients at day 3 to day 24 after the onset of illness, although the signal was relatively weak in fecal samples (22). These results suggest that antigen-captured assay could be useful for the early diagnosis of SARS-CoV infection.

We developed an antigen-capture ELISA system that detects purified SARS-CoV virion at levels as low as 40 pg/mL. The sensitivity of the system, which comprised two anti-N mAbs, seems high enough to detect virus protein in patient sera when compared to a recently reported antigen-capture ELISA system, which detects 100 pg/mL of purified recombinant N protein, successfully determined the virus protein in patient sera (22). We are now improving the sensitivity of the system and checking its applicability in the diagnosis and monitoring of SARS-CoV infection. Although none of our mAbs cross-reacted to human or other animal coronaviruses (229E, TGEV and MHV) by ELISA, it is also important to define the specificity of these mAbs by other techniques such as Western blot and immunofluorescent staining. This issue is currently under investigation.

Two anti-S mAbs, SKOT-19 and -20 demonstrated significant virus neutralizing activity. It would be interesting to address whether these mAbs interfere with the binding of the virion to its recently reported receptor, ACE2 (27). If this were the case, the humanization of these mAbs by means of either CDR-grafting or mouse-human chimeric antibody would be of interest as a possible application for the therapeutic use of these mAbs.

ACKNOWLEDGMENTS

We are grateful to Ms. Sayuri Yamaguchi for her assistance in establishing hybridomas.

This work was supported by grant from the Ministry of Health, Labour and Welfare of Japan.

REFERENCES

1. Drosten, C., Gunther, S., Preiser, W., van der Werf, S., Brodt, H. R., Becker, S., Rabenau, H., Panning, M., Kolesnikova, L., Fouchier, R. A., Berger, A., Burguiere, A. M., Cinatl, J., Eickmann, M., Escriou, N., Grywna, K., Kramme, S., Manuguerra, J. C., Muller, S., Rickerts, V., Sturmer, M., Vieth, S., Klenk, H. D., Osterhaus, A. D., Schmitz, H. and Doerr, H. W. (2003): Identification of a novel coronavirus in patients with severe acute respiratory syndrome. N. Engl. J. Med., 348, 1967-1976.
2. Ksiazek, T. G., Erdman, D., Goldsmith, C. S., Zaki, S. R., Peret, T., Emery, S., Tong, S., Urbani, C., Comer, J. A., Lim, W., Rollin, P. E., Dowell, S. F., Ling, A. E., Humphrey, C. D., Shieh, W. J., Guarner, J., Paddock, C. D., Rota, P., Fields, B., DeRisi, J., Yang, J. Y., Cox, N., Hughes, J. M., LeDuc, J. W., Bellini, W. J. and Anderson, L. J. (2003): A novel coronavirus associated with severe acute respiratory syndrome. N. Engl. J. Med., 348, 1953-1966.
3. World Health Organization (2003): Summary table of SARS cases by country, 1 November 2002 - 7 August 2003.
4. World Health Organization: WHO SARS international reference and verification laboratory network: policy and procedures in the inter-epidemic period.
5. Peiris, J. S., Chu, C. M., Cheng, V. C., Chan, K. S., Hung, I. F., Poon, L. L., Law, K. I., Tang, B. S., Hon, T. Y., Chan, C. S., Chan, K. H., Ng, J. S., Zheng, B. J., Ng, W. L., Lai, R. W., Guan, Y. and Yuen, K. Y. (2003): Clinical progression and viral load in a community outbreak of coronavirus-associated SARS pneumonia: a prospective study. Lancet, 361, 1767-1772.
6. Grant, P. R., Garson, J. A., Tedder, R. S., Chan, P. K., Tam, J. S. and Sung, J. J. (2003): Detection of SARS coronavirus in plasma by real-time RT-PCR. N. Engl. J. Med., 349, 2468-2469.
7. Cheng, P. K., Wong, D. A., Tong, L. K., Ip, S. M., Lo, A. C., Lau, C. S., Yeung, E. Y. and Lim, W. W. (2004): Viral shedding patterns of coronavirus in patients with probable severe acute respiratory syndrome. Lancet, 363, 1699-1700.
8. Chan, P. K., To, W. K., Ng, K. C., Lam, R. K., Ng, T. K., Chan, R. C., Wu, A., Yu, W. C., Lee, N., Hui, D. S., Lai, S. T., Hon, E. K., Li, C. K., Sung, J. J. and Tam, J. S. (2004): Laboratory diagnosis of SARS. Emerg. Infect. Dis., 10, 825-831.
9. Poon, L. L., Wong, O. K., Chan, K. H., Luk, W., Yuen, K. Y., Peiris, J. S. and Guan, Y. (2003): Rapid diagnosis of a coronavirus associated with severe acute respiratory syndrome (SARS). Clin. Chem., 49, 953-955.
10. Chen, W., Xu, Z., Mu, J., Yang, L., Gan, H., Mu, F., Fan, B., He, B., Huang, S., You, B., Yang, Y., Tang, X., Qiu, L., Qiu, Y., Wen, J., Fang, J. and Wang, J. (2004): Antibody response and viraemia during the course of severe acute respiratory syndrome (SARS)-associated coronavirus infection. J. Med. Microbiol., 53, 435-438.
11. Nie, Y., Wang, G., Shi, X., Zhang, H., Qiu, Y., He, Z., Wang, W., Lian, G., Yin, X., Du, L., Ren, L., Wang, J., He, X., Li, T., Deng, H. and Ding, M. (2004): Neutralizing antibodies in patients with severe acute respiratory syndrome-associated coronavirus infection. J. Infect. Dis., 190, 1119-1126.
12. Wang, W. K., Chen, S. Y., Liu, I. J., Chen, Y. C., Chen, H. L., Yang, C. F., Chen, P. J., Yeh, S. H., Kao, C. L., Huang, L. M., Hsueh, P. R., Wang, J. T., Sheng, W. H., Fang, C. T., Hung, C. C., Hsieh, S. M., Su, C. P., Chiang, W. C., Yang, J. Y., Lin, J. H., Hsieh, S. C., Hu, H. P., Chiang, Y. P., Yang, P. C. and Chang, S. C. (2004): Detection of SARS-associated coronavirus in throat wash and saliva in early diagnosis. Emerg. Infect. Dis., 10, 1213-1219.
13. Takasuka, N., Fujii, H., Takahashi, Y., Kasai, M., Morikawa, S., Itamura, S., Ishii, K., Sakaguchi, M., Ohnishi, K., Ohshima, M., Hashimoto, S., Odagiri, T., Tashiro, M., Yoshikura, H., Takemori, T. and Tsunetsugu-Yokota, Y. (2004): A subcutaneously injected UV-inactivated SARS coronavirus vaccine elicits systemic humoral immunity in mice. Int. Immunol., 16, 1423-1430.
14. Darnell, M. E., Subbarao, K., Feinstone, S. M. and Taylor, D. R. (2004): Inactivation of the coronavirus that